Department of Biomedical Research (DBMR), Murtenstrasse 50

Director: Prof. Dr. Mark Rubin

Supervisor: Prof. Robert Rieben

Co-Supervisor: Dr. Nicoletta Sorvillo

Ex Vivo vs In Vivo large animal model to study ischemia reperfusion injury in skeletal muscle following prolonged ischemia time

Masterthesis

Awarding the academic title

Master of Science in Biomedical Sciences

Submitted to the Medical Faculty of the University of Bern on 31.08.2021

Ahmed Fahiem Abdelsalam Emara (AE18b028)

von residence

Al Zanfaly st. – Al Santah, Al Gharbia – Egypt;

Bern, 3007, Switzerland

Declaration of Authorship

I herewith confirm that I wrote this thesis without external help and that I did not use any resources other than those indicated. I have clearly acknowledged all parts of the text where material from other sources has been used, either verbatim or paraphrased. I am aware that non-compliance with the above statement may lead to withdrawal of the academic title granted on the basis of this master's thesis by the Senate, according to the law governing the University of Bern.

Date:

signature of the student:

بِسْمِ اللَّـهِ الرَّحْمَـٰنِ الرَّحِيمِ

{وَمَا تَوْفِيقِي إِلَّا بِاللَّهِ ۚ عَلَيْهِ تَوَكَّلْتُ وَإِلَيْهِ أُنِيبُ} [هود من الآية:88]

صدق الله العظيم

Table of Contents

Table of Figures

1 Abstract

EX VIVO MACHINE PERFUSION TO ASSESS ISCHEMIA REPERFUSION INJURY OF AMPUTATED PORCINE LIMBS

Background

In limb replantation or -transplantation, reperfusion following ischemia induces a significant, paradoxical, injury to the graft with activation of, among other things, innate immune cells and the plasma cascade systems, leading to severe tissue damage. In this study, we aimed to develop an ex vivo – in vivo large-animal model to evaluate and compare the pathophysiology of ischemia/reperfusion (I/R) injury.

Methods

Surgically amputated forelimbs underwent 1h (control) vs. 9h of ischemia and were subsequently reperfused using an extracorporeal perfusion system (ex vivo, using whole, anticoagulated pig blood, both forelimbs used) or surgically replanted to the donor pig (in vivo, single forelimb used), aiming for 12h of reperfusion. Clinical data as well as blood and tissue samples were collected at different timepoints to analyze markers of muscle damage, endothelial cell and plasma cascade activation, as well as production of cytokines and growth factors.

Results

In the ex vivo reperfusion model, both ischemic and control limbs showed a higher pro-inflammatory reaction as compared to the in vivo situation. Moreover, ex vivo average reperfusion times were shorter and activation of coagulation and complement was more prominent, as well as the production of pro-inflammatory cytokines and muscle damage. Additionally, in both models, higher values of vascular growth factors were observed in 9h ischemic limbs as compared to controls and no difference was found for the anti-inflammatory IL-10. Furthermore, higher levels of E-selectin expression were found in controls vs. 9h ischemic limbs.

Conclusions

Our preliminary results suggest that I/R injury can clearly be detected in an ex vivo reperfusion setting with whole blood. That this injury was apparently stronger ex vivo may be due to the additional pro-inflammatory and pro-coagulant effect of the ex vivo perfusion setting itself. As the activation pattern in vivo and ex vivo is comparable, we conclude that the use of an ex vivo system to assess strategies to prevent I/R injury in limb replantation, and potentially also in VCA and organ transplantation, is favorable and has a better 3R profile because both forelimbs of the animal can be used simultaneously.

2 Introduction & Aim

2.1 Traumatic limb amputation

Extremities' amputation are devastating injuries, which lead to both aesthetic and functional impairment of the body, as well to the accompanied psychological and socioeconomic burden. Based on demographic analysis, the prevalence of extremity amputation in USA was estimated at 1.6 million in the year 2005 with a projected estimate to more than double (3.6 millions) by the year 2050 [1]. Meanwhile in Europe, one analysis estimated the prevalence among Norwegian population of 11.6 per 100,000 adults [2]. Extremities' amputation can occur for instance as secondary to diabetic neuropathies (e.g. diabetic foot), vascular disorders (e.g. thrombi), bone malignancies or because of traumatic injuries, with the latter being the leading cause of upper limb amputations. In contrast, lower limbs amputations are common secondary to co-morbidity such as diabetes and vascular dysfunction.

Traumatic limp amputation is a common incident among men with age between 15-45 years old. Higher incidences are seen distally (below wrist or toe amputation) owing mainly to occupational and industrial accidents with sharp objects. Based on the form of injury, traumatic limb amputations can vary from a severe form of damage –caused by crush or avulsion injury– to a lesser form caused by sharp objects, also known as blade injuries. Additionally, the type of trauma –among other factors– carries an important weight in determining whether to sacrifice the limb or to attempt for replantation [1].

Replantation is defined as the surgical attempt to reattach a detached body part. The first reported limb replantation surgery was conducted in 1962 by Malt and McKhan after successfully replanting an amputated forearm of a 12 years old boy who suffered a train accident [3]. The following five decades has seen a rise of successful replantation surgeries thanks to the technical and procedural advancements (e.g. microsurgery). In the early years, the main goal of replantation was to maintain a viable tissue. However later on, the main outcome of replantation has shifted towards retaining both the viability and, most importantly, the functionality of the amputate. As stated by the Chinese surgeons in 1973 "survival without restoration of function is not success", while sharing their clinical expertise in pioneering several surgical techniques in the field of replantation [4].

In clinical setting and similar to any trauma case, the main priority is to resuscitate the amputee through the initial ABCDE assessment. In brief, this indicates maintaining an intact airway and ensure breathing, volume resuscitation and homeostasis, wound debridement, and finally assessing for associated injuries. Meanwhile, the amputated extremity is wrapped in dry,

sterile gauze, and maintained in a cold storage. Afterwards, surgeons are faced with the challenging decision of whether to attempt for replantation or proceed with amputation. Several factors are considered before the decision of replantation. On the amputee side, these variables include age, comorbidities, insurance coverage, access to physiotherapy, availability of intensive care unit and skilled surgeons, and, most importantly, the psychological readiness for the long recovery process. Other variables related to the amputate include mechanism of injury, site of amputation, extent of damage and the duration of ischemia. In general, young age, absence of comorbidities, blade injuries, short ischemia time and distal amputations are all indications of favorable replantation outcome. Nonetheless, clinical algorithms are now in place for a systematic management towards the extremities' amputation [5].

Among the aforementioned variables, ischemia time carries a big impact on the outcome of replantation. Different tissue types can sustain different ischemia times before an irreversible damage takes place. Bone, nerve, and skin tissue has longer ischemia tolerance compared to muscle mainly due to the higher metabolic activity of the latter. The indicated ischemia tolerance for muscle tissue is up to 6 hours of warm ischemia and 12 hours of cold ischemia [5]. Several articles have been published reporting successful replantation following a protracted ischmia time. Namely, digits' replantation following 33h of warm ischemia [6] and up to 94h of cold ischemia [7], and hand replantation after 33h of warm ischemia [8-9]. Additionally, success rate of 64% [6] and 67% [9] have been reported for hand and digits replantation after extended ischemia time. Contrariwise, replantation of proximal amputations involving a large muscle volume are avoided [10]. Owing to a paradoxical phenomena –induced upon revascularization– known as ischemia-reperfuison injury (IRI).

2.2 Ischemia-Reperfusion Injury (IRI)

Ischemia-reperfusion injury is a paradoxical tissue injury orchestrated through a series of pathophysiological events, initiated by the ischemia-related injury, followed by an aggravated damage and cellular death upon reperfusion. Different events take place during ischemia time and upon reperfusion.

2.2.1 Pathophysiology during ischemia & reperfusion

A state of ischemia results when the blood supply to tissue fails to meet the oxygen and nutrients' demands required to maintain its metabolism. During homeostasis, cellular metabolism relies on the aerobic metabolism of glucose known as aerobic glycolysis. This process is initiated with the split of glucose into pyruvate, which is then translocated into the mitochondria. Thereafter, pyruvate is utilized in a series of oxidative phosphorylation known as Krebs cycle, followed by an electron transport chain, and yielding a sum of 34 ATP molecules generated. In a state of hypoxia (lack of oxygen), only glycolysis can take place leading to

pyruvate accumulation in the cytoplasm which in turn is converted to lactic acid. Comparatively, this process yields only 2 ATP molecules. Therefore, ischemic cells suffer from both low energy (ATP shortage) and low PH (lactic acidosis). The lack of ATP production leads to disruption of the active ion-exchange pumps namely Na^+/K^+, Na^+/H^+ on the cell membrane side and $Ca^{2+}/ATPase$ on the endoplasmic reticulum membrane. The so forth accumulation of Na^+, Ca^{2+} and H^+ in the cytoplasm will cause further acidosis in addition to hyperosmolarity, water retention, and cellular swelling [11].

The generated ATP molecules are first metabolized into Inosine-monophosphate, then hypoxanthine. Hypoxanthine is converted afterwards into xanthine and finally into uric acid by the xanthine oxidoreductase enzyme complex. This process leads to the production of either NADH by xanthine dehydrogenase or superoxide (O_2-) –a precursor to secondary Reactive Oxygen Species (ROS) e.g. Hydrogen peroxide H_2O_2– by xanthine oxidase. Furthermore, the state of hypoxia, in addition to cytokines and the mitochondrial calcium-activated calpain, induce the proteolytic conversion of xanthine dehydrogenase into xanthine oxidase [11]. As a result, the abundance of hypoxanthine and xanthine oxidase in ischemic tissue will lead to ROS overproduction once circulation is restored. Moreover, the accumulated ROS will induce lipid peroxidation of the cellular membrane resulting in production of pro-inflammatory eicosanoids and eventually cell death. Besides xanthine oxidase, other mechanisms contribute to ROS production namely mitochondrial electron transport chain, NADP oxidase and uncoupled NOS system [13].

2.3   IRI in skeletal muscles

The debilitating contribution of Ischemia-reperfusion injury has been recognized in several pathologies involving different organs like heart, brain, kidney, intestine and skeletal muscles. For instance in acute coronary syndrome, pulmonary embolism, stroke, sleep apnea, organ transplantation and major vascular surgeries. In 1926, an experimental study was conducted in dogs to investigate ischemic contracture and edema formation accompanying tourniquet application [12]. It is probable this was the first documentation of IRI of skeletal muscle in literature.
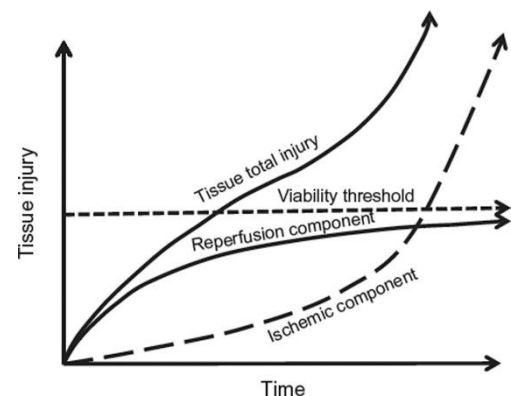
Figure 1 Components of IR tissue injury. Total tissue injury is the sum of damage incurred during and by ischemia and the additive damage inflicted upon reperfusion onwards [13].

2.3.1 Muscle damage

The extent of IRI is mainly influenced by the tissue susceptibility to ischemia-related damage, ranging from highly susceptible e.g. brain and heart to far less susceptible e.g. cornea. In skeletal muscle, ischemia-related damage occurs as early as 3h and reaching an irreversible and extensive damage nearly by 6h of ischemia time [13]. The inflicted tissue damage caused by IRI is divided into ischemia-related and reperfusion related injuries.

Different mechanisms of cellular death are involved in IRI including apoptosis, necrosis, necroptosis and autophagy. Apoptosis is a form of programmed cell death, which may involve a crosstalk between its extrinsic (mediated by death ligands) and intrinsic pathways (mediated by mitochondria). Both pathways employ the downstream activation of caspase cascade system, which then results in cell death via proteolysis. Contrariwise, necrosis is an unregulated form of cell death which is manifested by excessive cellular stress and leading to cellular swelling and rupture. Likewise, Necroptosis is a form of necrosis; however regulated through Receptor-Interacting Proteins (RIP1/RIP3) which later form necrosoms and induce cell suicide. On the other hand, autophagy is a regulated mechanism to clear out damaged or dysfunctional cellular components by surrounding it into vesicles, which later on, fuse with lysosomes for degradation [13].

In IRI of skeletal muscle, a study conducted by Cowled *et. el.* in rats has shown that apoptosis had a minor contribution to the inflicted muscle damage of IRI [14]. Additionally, histological examination showed that tissue damage was evident mainly during ischemia time not reperfusion and apparent edema formation following the latter [14].

2.3.2 Endothelial cell (EC) activation & Leukocytes' trafficking

Six decades ago, Willms-Kretschmer has shed the light on the biological role of endothelial cells –besides being the vessel internal lining– while studying the vascular changes in contact dermatitis [15]. Not long after, several studies have documented different biological events taking place in endothelial cells, including transcriptional, morphological and secretory events, which were referred to as endothelial cell activation [16]. Such events include the secretion of von-Williberand factor (vWF) and chemokines, expression of plasminogen activator inhibitor-1 (PAI-1), and upregulation of surface adhesion molecules e.g. ICAM-1, VCAM-1, E-selectin.

Endothelial cells plays an important role in immune cell trafficking and emigration to injury sites, through a group of transmembrane adhesion molecules named selectins. For instance, P-selectin, E-selectin and L-selectin. P-selectin is continuously expressed on the surface of EC and platelets. Contrariwise, E-selectin expression is induced on the surface of EC by certain stimuli e.g. TNF-α. Furthermore, E-selectin essentially binds L-selectin on the surface of leukocytes to enhance their rolling against the vessel wall [17].

The role of neutrophils in aggravating IRI is well recognized [20]. The additive damage of neutrophils was presented as higher vascular permeability and edema formation, and larger muscle infarction size. This is ought to the additional ROS production by neutrophils following their recruitment and activation [18]. In addition, neutrophils' additive damage is mediated through capillary plugging and no-reflow phenomena during reperfusion [19]. In IRI of skeletal muscle, neutrophils trafficking and activation is enhanced by cytokine and chemokine secretion in addition to the upregulation of selectins and cellular adhesion molecules on EC surface. Attenuation of IRI damage was observed in studies using antibodies against selectins namely P-selectin, L-selectin, E-selectin [21-23].

2.3.3 Cytokines and growth factors release

Hypoxia plays an essential role in different diseases promoting inflammation, influencing innate and adaptive immunity, and facilitating cancer progression. In a gene analysis study conducted in mice following the ligation of femoral artery, the analysis of transcriptome revealed upregulation of genes mediating inflammation and downregulation of genes controlling muscle function [24]. Further to its metabolic derangement role in ischemic tissue, hypoxia promotes a state of inflammation and angiogenesis through a cascade of oxygen-sensitive hydroxylases, which then promote the expression of NF-κB and hypoxia-induced factors (HIFs). As a result, inducing several cytokines and growth factors including interleukin-6 (IL-6), interleulin-8 (IL-8), interleukin-1β (IL-1β), tumor necrotic factor-alpha (TNF-α), vascular endothelial growth factor (VEGF) and platelets derived growth factor (PDGF) [25].

2.3.4 Role of Complement cascade

Complement cascade system is a highly conserved and a major player of the innate immune defense mechanisms. This cascade system comprises of three different pathways and several molecules participating in the initiation (e.g. C1w), or amplification process (e.g. C3), or mediating complement injury (e.g. MAC). Yet all three pathways and processes converge to a one final product known as membrane attack complex (MAC). As illustrated in figure 2, Complement cascade can be activated through the classical, lectin and alternative pathways. Classical pathway starts with the binding of immunoglobulins to an antigen which is then joined by C1q molecule to form the C1 complex. The formed complex acts on C2 and C4 proteins cleaving them to C2a+C2b and C4a+C4b, respectively. Both C4b and
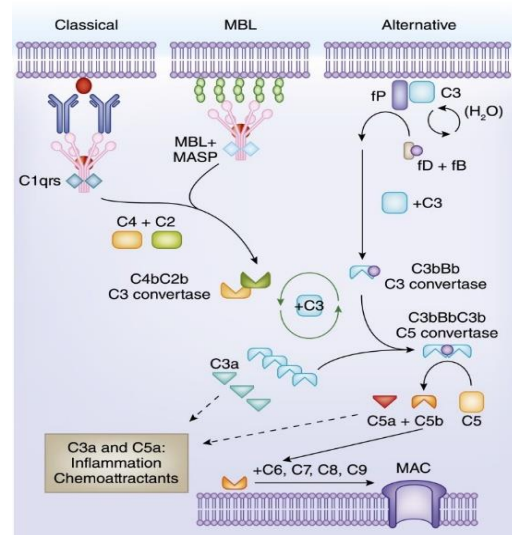
Figure 2 Complement cascade pathways. Three pathways and several proteins involved promoting cell lysis through MAC and inflammation through C3a and C5a chemoattractant capacity [26].

11

C2b join to form C3 convertase, which later cleaves C3 protein into C3a+C3b. Similarly, cleaved molecules –from both classical and alternative pathways- join together to form the C5 convertase, which results in C5a+C5b. Afterwards, C5b molecule binds to other complement proteins namely C6, C7, C8 and C9 to form MAC, which is thereafter forms pores in the cellular membrane and promotes cell lysis [26]. In addition, cleavage of C3 molecule can take place spontaneously in plasma through the alternative pathway. In contrast, lectin pathway is initiated through the binding of mannose binding lectins (MBL) to pathogens. However, both classical and lectin pathways lead to the formation of C3 convertase (C4bC2b), similarly.

The role of complement cascade in aggrevating IRI-associated damage has been well-studied. A study of hindlimb IRI in mice deficient from C3 and C4 demonstrated protection in these mice against reperfusion injury [27]. As well, other studies highlighted the protective effect following the blockade of complement pathways. Earlier studies suggested that complement activation is mediated solely through the activation of the classical pathway [28-30]. These studies demonstrated protective effect in immunoglobulin-deficient animal model [31], also reconstituted the injury with normal sera. This finding sparked further investigation of the implied antigen-antibody trigger of the classical pathway. Shortly after, Zhang et el. [32] identified a neoantigen, known as non-myosin heavy chain NMHC-II, which binds to circulating natural IgM propagating the classical pathway. Moreover, recently, the theory of self-antigen was backed by Shi et el. [33] who demonstrated the binding of natural IgM to actin muscle fibers. Furthermore, Zhang et el. [34] showed that natural IgM antibodies also mediate complement activation through the lectin pathway. The role of lectin pathway in complement-mediated IRI injury was also supported by Chan et el. [35] using MBL-deficient mice, which were protected from reperfusion injury following skeletal muscle ischemia.

2.4   Aim of the study

The aim of this study is to establish and evaluate IRI in a large animal model of major limb amputation both with machine perfusion (*Ex Vivo*) or surgical replantation (*In Vivo*) following a prolonged normothermic ischemia time of 9 hours. We speculate a stronger manifestation of IRI response among the *In Vivo* compared to *Ex Vivo* group.

3 Materials & Methods

3.1 Project design

Surgically amputated porcine forelimbs were exposed to either ≤1h or 9h of ischemia at room temperature (22°C) and baseline blood and muscle tissue samples were collected (Figure 3.I). Following ischemia, amputated limbs were reperfused for 12 hours either by using an extra-corporeal circulation (Ex Vivo) or by replantation to the donor (In Vivo). Hourly clinical monitoring and timepoints-defined blood sampling were performed during reperfusion. At Endpoint (EP), tissue samples were collected from muscles of the reperfused limb, as well from liver, lung and kidney exclusively in the In Vivo group (Figure 3.II).
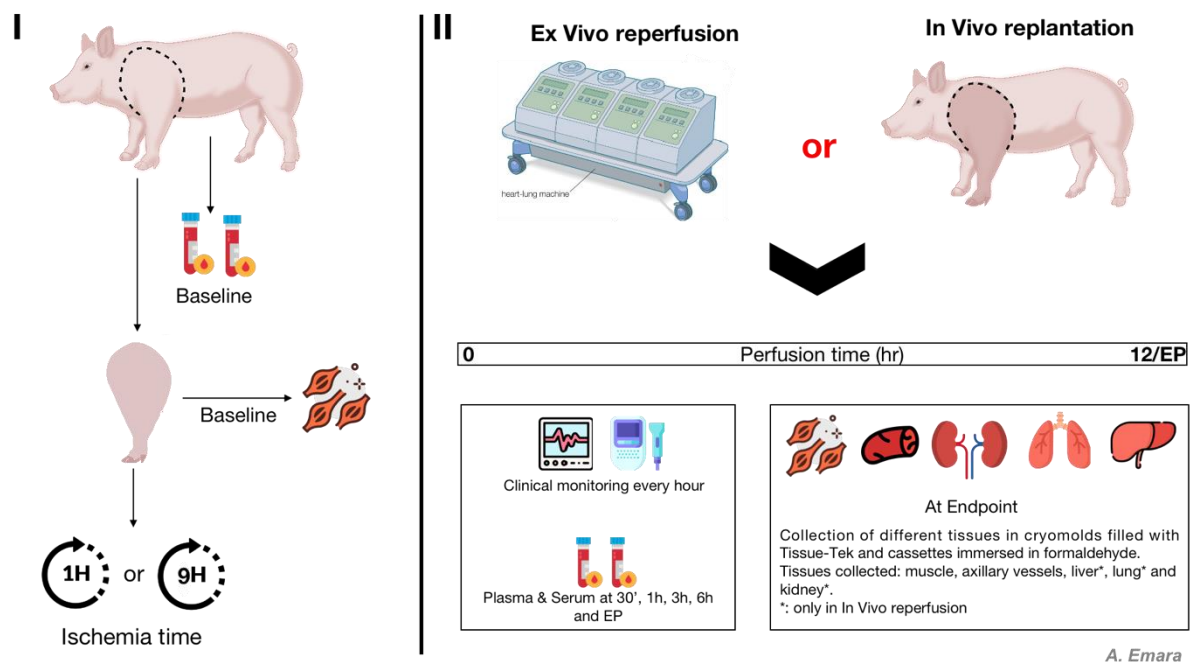
Figure 3 Overview of the experimental design (own illustration).
Pigs were sedated and general anesthesia was induced to commence with the amputation surgery. Baseline plasma and serum samples were collected, and forelimb amputation was performed. Thereafter, collection of baseline muscle samples and limb weight measurement followed by a dedicated warm ischemia time (I). Amputated-ischemic forelimbs were then perfused for 12h, using a heart-lung machine, or surgically replanted to the donor pig. Hourly clinical monitoring and timepoint-wise blood sampling was conducted until endpoint. Hereafter, euthanasia or cessation of machine perfusion took place followed by endpoint sampling of plasma, serum, muscle and organs (II), and storage until future analysis.

3.2 Surgical procedure

3.2.1 Animal Subjects

Out-bred pigs weighing 40-50 kg were housed in the farm of origin. Adequate health check was carried out at the nearby veterinary hospital to rule out any underlying pathology that may contradict or affect the surgical model e.g. heart or lung conditions. Pigs were excluded from the cohort if pigs were deemed unfit for surgery due to a pathological condition. Additionally, pigs were fasted 8h before surgery and only to water was provided.

3.2.1.1 *Ex Vivo* groups (1h and 9h ischemia)

Eight surgical experiments were performed for *Ex Vivo* perfusion. The right forelimbs were assigned to 9h of ischemia (ischemic group) and left forelimbs were assigned to ≤1h of ischemia (Surgical controls). Eight surgical experiments were conducted. We used the first 4 forelimbs (the first 2 surgical experiments) to re-establish the surgical technique and machine perfusion protocol. Therefore, only 6 forelimbs in each group were compared and data of the first 2 surgical experiments were excluded (n=6 in both groups).

3.2.1.2 *In Vivo* groups (1h and 9h ischemia)

Out of 7 planned experiments per each group, a total of 6 experiments were performed for the 1h ischemia group and 5 experiments for the 9h ischemia group until April 2021. Experiments of both groups were conducted in a random order based on feasibility and available resources during the pandemic. The first experiment of 1h ischemia group was performed to re-establish the replantation and vascular anastomosis technique, and therefore was excluded from analysis. For the timespan of my thesis, only 3 pigs were analyzed and included in my comparisons: pigs 2-4 from the 1h ischemia group and pigs 1-3 from the 9h ischemia group.

A sample size of n=6-8 in each group was calculated by power analysis based on accumulated data from previous studies. The experiments are thus still ongoing. A total number of 10 experiments was approved by the cantonal authorities in Bern (permission no. BE65/19), in order to account for any unforeseen procedural failure. Animal experimentation was conducted in line with the national animal-welfare guidelines and laws.

3.2.2 Forelimb Amputation

Our surgical model has been described previously [36]. In brief, pigs were sedated using an intramuscular cocktail of ketamine, methadone and dexmedetomidine to achieve adequate sedation. A venous canula with a crystalloid solution was established and general anesthesia was induced using intravenous administration of propofol and ketamine. Next, pigs were intubated, and mechanical ventilation was set to PEEP mode aiming for a $PaCO_2$ of 40-45 mmHg. Thereafter, isoflurane inhalation was used to deepen and maintain general anesthesia at an adequate level, across the whole duration of the experiment. Subsequently, a urinary catheter was inserted, and access to a central artery and vein was established.

An inverted Y-shaped demarcation line was drawn around the forelimb including the scapula. and an intravenous bolus of heparin (10,000 IU) was administered. Next, dissection of skin and shoulder girdle muscles was initiated using an electrocauterization device (ERBE ICC 350, ERBE Elektromedizin GmbH, Tuebingen, Germany) until the axillary vessels and nerve were identified. Blood flow in the axillary artery was measured using a flowmeter (T206, Transonic Systems, Ithaca, NY), axillary vessels were then ligated, and amputation of the forelimb was completed. Afterwards, the amputated forelimb was wrapped in a sterile bag and baseline weight was measured.

In *Ex Vivo* groups, both forelimbs were amputated starting first with the right forelimb – which was assigned to 9h ischemia – followed by another I.V bolus of heparin (5000 IU) and the left forelimb was amputated thereafter.

During ischemia time of the *In Vivo* 9h ischemia group, amputated forelimbs were kept at room temperature (approximately 22°C) in a sterile bag until the start of replantation. Meanwhile, we used the EpiGARD (Biovision GmbH, Ilmenau, Germany) wound dressing to protect the defected skin area at the amputation site. Owing to the short ischemia time of the *In Vivo* 1h ischemia group, replantation procedure commenced immediately after baseline limb-weight measurement was recorded.

3.2.3 Ex Vivo Perfusion (Heart-Lung Machine Perfusion)

3.2.3.1 Machine perfusion (Figure 4a & 2b)

Following the amputation of the second forelimb another 2500 IU of heparin were administered. Blood was then collected into two bags, preloaded with 10,000 IU of heparin each; with a blood amount of 600 ml in each bag; and bags were stored at 4°C until the start of perfusion. Afterwards, pigs were immediately euthanized.

At the end of the respective ischemia time for each group, the vasculature of the ischemic limbs was rinsed through the cannulated axillary vessels using hydroxyethyl starch (HAES, Voluven, Fresenius) to remove any residual blood and accumulated metabolites.

We used 250 ml of HAES to prime the extracorporeal circuit of the heart-lung machine (Figure 2a). Amputated limbs were then connected to the circuit through the cannulated vessels and perfused using autologous heparinized blood (Figure 2b). After 1h of perfusion, a bolus of 40mg Solumedrol was added to the circulation to counteract the no-reflow phenomena. Blood leaking from the amputated forelimbs was collected in a sterile bag during perfusion and added back into the circuit. Circulating autologous blood was maintained at a temperature of 37°C using a heater-cooler unit (HCU30; Maquet GmbH and Co. KG, Rastatt, Germany), along with an oxygenator (MEDOS Hilite 800 LT; Medos Medizintechnik AG) to adjust blood oxygenation based on arterial blood gas measurements.
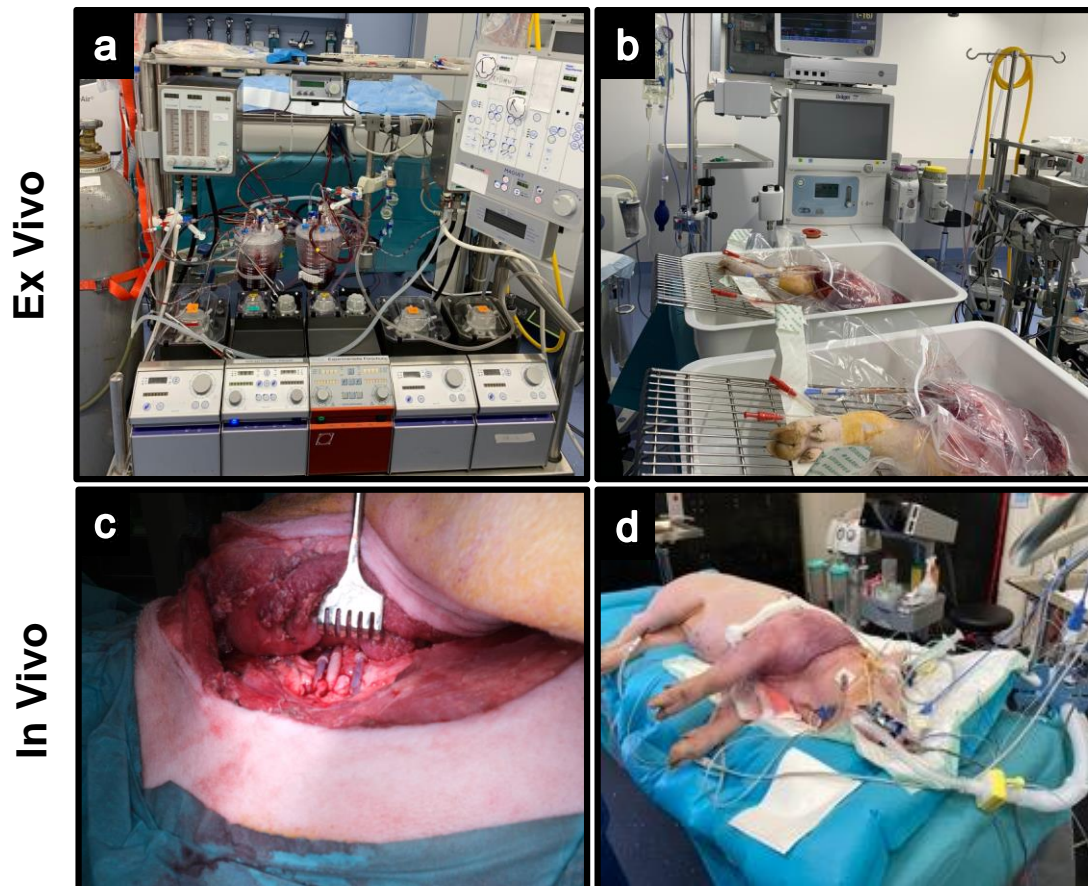
Figure 4. Demonstration of the Ex Vivo and In Vivo perfusion experiments.

(a) A heart-lung machine setup during *Ex Vivo* perfusion experiments. (b) Amputated and cannulated forelimbs wrapped in a sterile bag during ischemia time. (c) Intact axillary vessels' anastomosis during an *In Vivo* replantation. (d) An on-going *In Vivo* reperfusion of a replanted forelimb (9h ischemia group) under a state of general anesthesia.

3.2.3.2 Monitoring

During machine perfusion, several parameters were recorded including blood oxygenation, perfusion rate (targeted at 100-200 ml/minute) and pressure (targeted above 55 mmHg), limb carpal temperature and compartment pressure. Limb perfusion was assessed at different intervals using a Laser Doppler flowmetry (EasyLDI Perfusion Camera, Aïmago SA). Besides, blood gases and electrolytes were measured at baseline and hourly during perfusion. Electrolytes and pH imbalances were corrected based on an established protocol. Moreover, Activated Clotting Time (ACT) was monitored, and circulating blood was maintained at a full heparinization state (ACT >999 seconds).

3.2.3.3 Endpoint

The *Ex Vivo* perfusion protocol was carried out aiming for 12h duration of reperfusion. Machine perfusion was early terminated in the case of:

1- Clot formation in the limb manifested as elevated perfusion pressure or
2- Excessive blood leakage into the tissue (e.g. edema formation or tissue hemorrhage) impairing limb perfusion due to the progressive lack of perfusate blood.

3.2.4 In Vivo Perfusion (Replantation)

3.2.4.1 Replantation procedure (Figure 4, c & d)

At the start of replantation, subcutaneous sutures were used to hold the amputated forelimb in place in order to reconnect the axillary vessels. We used Prolene 4.0 sutures to anastomose the ends of the axillary artery, and a venous Coupler 4.0 mm (Synovis Micro Companies Alliance, Inc., Birmingham, AL) for axillary venous anastomosis (Figure 2.c).

Following anastomosis of the vessels and before the start of perfusion, a bolus of heparin 80IU/kg was administered intravenously, and then clamps were removed to restart circulation into the replanted limb. Arterial blood flow was measured again in the axillary artery and mean arterial blood pressure was recorded. Afterwards, the replanted forelimb was fixed in place using muscle and subcutaneous sutures. A drainage (Redon 14Ch) was inserted, and skin stapler was used for skin closure. Lastly, compartment pressure was recorded at the dorsal group of distal muscles (flexors), and the measurement needle was fixed in place for continuous recording of compartment pressure.

3.2.4.2 Monitoring

In contrast to *Ex Vivo* setup, several parameters were closely monitored in *In Vivo* both during ischemia and reperfusion time. These parameters included heart rate, respiratory rate, oxygen arterial saturation, systemic temperature (nasal), blood pressure (invasive), and urinary

catheter output. As well, general anesthesia and nociception were closely monitored through brain EEG activity and stimulatory tactile and pain reflexes.

Additionally, Mean Arterial Pressure (MAP) was targeted at 70 mmHg using vasopressors, and respiration was maintained on a volume-controlled mode using PEEP ($PaCO_2$ target: 40-45 mmHg). Arterial Blood Gases (ABG), blood pH and electrolytes were measured at different intervals and correction was carried out based on a pre-defined algorithm developed by the anesthesia team. Lastly, Activated Clotting Time (ACT) was targeted at twice the baseline value using continuous heparin infusion.

Meanwhile perfusion, additional parameters were recorded including compartment pressure – both ipsilateral and contralateral– and limb carpal temperature. Assessment of limb perfusion was hourly performed using both a Laser Doppler flow meter (EasyLDI Perfusion Camera, Aïmago SA) –in both *Ex Vivo* and *In Vivo* limbs- and/or a hand-held doppler (unidirectional Doppler D900, KS Medizintechnik, Germany), only for the *In Vivo* group.

3.2.4.3 Endpoint

We defined the endpoint of reperfusion as the occurrence of:

1- reaching 12h duration of reperfusion with no complications that indicate early termination and euthanasia or
2- Clot formation in the limb vasculature preventing further limb perfusion (manifested clinically e.g. limb swelling, cyanosis, loss of peripheral pulse...etc.)
3- A systemic inflammatory response leading to Multiple Organ Dysfunction (MOD), as a consequence of IRI.

3.2.5 Euthanasia

Before euthanasia, the endpoint blood sample was obtained, and the replanted forelimb was then re-amputated. To euthanize, we used an intravenous overdose of pentobarbital (100mg/kg) until a flat EEG and asystole (ECG) was recorded. Hereafter, a midline incision was performed and organ tissue samples were collected (figure 1II).

3.3 Sample collection and storage

Blood collection and tissue sampling took place at baseline and at predefined time points during the experiment. Blood was collected once a central arterial line was placed. Baseline muscle sample was collected from the adjacent muscle area to amputation site and distant from any electrocauterized areas. During reperfusion time, blood sampling took place at 30', 1h, 3h, 6h, 9h and endpoint of reperfusion. Following euthanasia, tissue samples were collected from liver, kidney and lung in addition to muscle.

3.3.1 Blood Collection

At each timepoint, Blood was collected in 5ml serum and EDTA tubes. Serum tubes were left for 30 minutes at room temperature to allow blood clotting. Meanwhile, EDTA tubes were centrifuged at 1000 G speed, 4° C for 20 minutes and similarly for serum tubes. After centrifugation, plasma and serum were aliquoted into 1.5ml Eppendorf tubes; 500uL each. Eppendorf tubes were placed in a box of dry ice to allow rapid freezing then samples were organized in a box and transferred to -80°C freezer until analysis.

3.3.2 Tissue Collection

Muscle and organ tissue were embedded in disposable plastic cryo molds filled with Optimal Cutting Temperature (O.C.T) medium. Muscle samples were collected from proximal and distal muscles in relation to the amputation site. In addition, muscle samples were embedded both in a longitudinal and transverse direction based on the orientation of muscle fibers. After embedding, cryo molds were then placed on a surface of crushed dry ice to allow for rapid freezing, and to minimize ice-crystals formation.

In addition to cryo-preservation, formaldehyde-fixed tissue samples were collected in tissue cassettes submerged in a container filled with 4% formaldehyde, and delivered to the pathology lab for a histological (H&E) analysis.

Furthermore, ten muscle punch biopsies were obtained from different areas in the limb, then placed in a pre-weighed petri dish. The weight of petri dishes were again recorded and petri dishes were placed inside an 80 oven. After a duration of 40h, a final weight was recorded to derive the wet/dry ratio.

Lastly, additional muscle tissue samples were collected into 1.5 ml cryotubes, snap frozen in a box of dry ice and stored at -80°C until analysis' time.

3.4 Immunofluorescence

3.4.1 Cryosections

Frozen muscle cryo molds were transferred from -80°C to -20°C one hour before cutting. Cryosections of 5 µm were made using a microtome (Thermo Scientific Microm HM 560 Cryostat-Series). Sections were then placed on labeled slides, and left to air dry for 30-60 minutes. Afterwards, a staining protocol was performed, or slides were transferred back into -80°C until further analysis.

3.4.2 Immunostaining Protocol

Following air drying, tissue samples were fixed for 10 minutes by submerging slides in a jar filled with a cold mix (–20°C cold) of acetone-methanol (1:1 dilution). Slides were then transferred into another jar filled with Tris-HCl Buffered Saline (TBS) –prepared from TBS 20x stock and diluted using ultra-pure H_2O– and re-hydrated on a shaker for 15 minutes. Next, we used a cotton swap to dry around the tissue specimen and boundaries were marked using a Dako pen (Dako, cat: s-2002). Next, tissue specimens were covered by a solution of TBS-5% BSA and incubated for one hour, to prevent non-specific binding antibodies (ab). After incubation, blocking solution was removed by tapping slides on a piece of tissue paper. A pre-defined mixture of primary ab was prepared and applied thereafter.Afterwards, tissue specimens were incubated overnight at 4°C, and protected from light when required.

On the following day, ab solution was removed, and slides were triple (3x) washed in TBS solution for 15 minutes each time. Next, specimens were covered by the secondary (2ry) ab mixture and incubated for one hour at room temperature. Slides were protected from light during incubation time of secondary ab and primary ab, if fluorochrome-labeled. After incubation, slides were triple washed in TBS on a shaker, for 20 minutes each time. Afterwards, slides were dried out using a stretching table at 40°C or tissue paper. A mounting medium (ProLong Gold Antifade mountant, P36934, Thermo Fisher Scientific Inc.) was applied thereafter and cover-slides were fixed using a transparent nail polish.

This protocol was optimized following several tests in order to obtain a better signal with minimal background noise. Throughout the staining protocol, tissue specimens were maintained wet until the mounting step. Tissue specimen for all experiments were immunostained simultaneously to minimize any confounding. Lastly, 1ry and 2ry antibodies (table1, table2) used in our protocol were tested before and signal specificity was ensured.

3.4.3 Imaging & Analysis

Images were acquired using a confocal microscope (Carl Zeiss microscope LSM 710 and LSM 880). Acquisition settings for each marker (e.g. CD31) were maintained across all slides of comparison. A minimum of 5 images at 20x magnification were obtained spanning different areas within each tissue specimen.

Image analysis was performed using Fiji software, version 2.1.0/1.53c. First, a signal-intensity threshold was determined by using the auto-threshold function provided in the software. Several images with a strong signal were analyzed to determine the cutoff threshold for background elimination. Next, the defined threshold value was applied to all images. Afterwardss, Measurement of signal intensity was set to the assigned threshold-value. Lastly, output measurements were recorded including mean gray value, area and integrated density.

Table 1 Primary antibodies used for immunofluorescence staining. * is a FITC labeled antibody. Antibodies were diluted in a prepared solution of TBS + 1%BSA + 0.05% Tween 20.

Marker	Company	Catalog #	Species	Type	Dilution
PECAM-1 (CD31)	R&D systems	MAB33871	Rat anti Pig	Monoclonal	1:100
Dystrophin	Abcam	Ab15277	Rabbit anti Human	Polyclonal	1:200
E-Selectin (CD62E)	Santa-Cruz	SC96847	Mouse anti Pig	Monoclonal	1:100
Complement (C3b-c)*	DAKO	F0201	Rabbit anti Human	Polyclonal	1:100
Anti IgM*	Mybiosource		Goat anti Pig	Monoclonal	1:250
Macrophages (CD68)	Bio-Rad	MCA2317GA	Mouse anti Pig	Monoclonal	1:100
Fibrin(ogen)*	R&D systems	F0111	Rabbit anti Human	Polyclonal	1:100

Table 2 <u>Secondary antibodies used for indirect immunofluorescence staining.</u> Antibodies were diluted (1:500) in a prepared solution of TBS + 1%BSA + 0.05% Tween 20.

Host Species	Catalog #	Reactivity	Fluorochrome
Donkey	A32766	Mouse	Alexa Flour 488
Donkey	A21208	Rat	Alexa Flour 488
Goat	A11034	Rabbit	Alexa Flour 488
Goat	A11077	Rat	Alexa Flour 568
Donkey	A10037	Mouse	Alexa Flour 568
Donkey	A10042	Rabbit	Alexa Flour 568

3.5 <u>ELISA</u>

Several markers were quantified in plasma and serum samples using the Sandwich ELISA principle on commercial kits. These markers include Plasminogen Activator Inhibitor-1/Tissue Plasminogen Activator (PAI-1/tPA) complex (#POPAITPAKT-COM, Molecular Innovations, Inc.), CKMM (catalog# CKMM9, Life diagnostics, Inc.), Complement component-3a (catalog# MBS2509360, MyBioSource, Inc.), D-Dimer (catalog# MBS7606777, MyBioSource, Inc.), Tissue Factor (catalog# MBS777903, MyBioSource, Inc.), soluble E-Selectin (catalog# MBS9718271, MyBioSource, Inc.) and Von-Willebrand Factor (catalog# MBS262909, MyBioSource, Inc.).

ELISA protocol was followed in line with the enclosed instructions of each kit. Before analyzing all samples, we tested several dilutions to determine the optimum dilution factor with Optical Density (OD) values ranged within the standard curve. Afterwards, all samples were analyzed as singlets on two 96-well plates in parallel.

In brief, plasma and serum aliquots were removed from –80°C and left to thaw on ice. Using the diluent in the kit, samples were diluted on an external 96well plate and standard was serially diluted based on the manufacturer's instructions. Diluted samples and standard serial dilutions were then incubated on each plate, standard dilutions in duplicate and samples in singlet. Following incubation, both plates were washed 3-5 times with the included wash buffer in line with each protocol. Next, plates were incubated with the diluted primary antibody followed by another washing step as instructed. Then, the included conjugated secondary antibody was diluted and incubated on each plate. Afterwards, plates were washed per instruction, and incubated with the substrate (TMP or HRP) in the dark. Lastly, substrate reaction was quenched by adding a stop solution and optical density was measured immediately after, using

a microtiter plate reader, and set to 450 nm absorbance. Per instructions, incubation steps took place either at room temperature or at 37°C, additionally, as well in a static condition or on a shaker. Sample concentrations were interpolated in contrast to standards' OD values and provided concentrations. Lastly, interpolated concentrations were multiplied by its dilution factor. Analysis was conducted using GraphPad Prism software version 9 (GraphPad, Sand Diego, CA, USA).

3.6   11-Plex assay (Bio-Plex multiplex suspension array)

Growth factors (VEGF, PDGF and bFGF), markers of inflammation (IL-6, IL-8, IL-10, MCP-1, IL-1β and TNF-α) and complement components (C5a and sC5b-9) were analyzed using an in-house multiplex suspension array (11-Plex) [37]. Briefly, fluorochrome-coded microbeads (Bio-Rad) were resuspended and activated. Microbeads were then coupled with the capture antibody using a Bio-Plex amine coupling kit (Bio-Rad, 171-406001). The antibody coupling process took place overnight at 4°C on a rotor and protected from light. The next day, beads were incubated with samples and standards for 60 minutes. Afterwards, beads were incubated with a biotinylated antibody for 30 minutes followed by a 10-minute incubation with Streptavidin-PE. Incubation steps took place on a plate-shaker and in the dark. Wells were also washed trice after each incubation step. Lastly, beads were resuspended in 100ul wash buffer and concentrations were measured in the Bio-Plex machine using Bio-Plex manager software V 6.0 (Bio-Rad). Plasma mesaurements of cytokines in several samples resulted in lower values beyond the range of the respective standard curve (Out Of Range-OOR). We thereby used the raw fluorescence intensity readings for statistical comparison.

3.7   Statistical analysis

Data analysis was performed using GraphPad Prism software version 9 (GraphPad, Sand Diego, CA, USA). Data obtained from plasma and tissue analyses, of *Ex Vivo* and *In Vivo* groups, are presented as a scatter plot with a line indicating the mean value. For both models, the development of each parameter was analyzed between groups (1h and 9h ischemia) at each timepoint (1h, 3h and EP), as well, within each group across the time of reperfusion.

In *Ex Vivo* groups, data was examined for normality distribution visually using Q-Q plot followed by Shapiro-Wilk test. In *In Vivo* groups –owing to the small sample size (n=3)– non-parametric tests were employed regardless the assumption of normality.

For the comparison between-groups, normally distributed data was analyzed using One-way ANOVA with Bonferroni post-test. Brown-Forsyth with Dunnet T3 post-test was used instead, if the Homoscedasticity assumption is violated (unequal variances). Elsewise, Kruskal-Wallis with Dunn's post-test was employed for non-parametric data. Similarly, for within-group analysis, a repeated-measures ANOVA with Tukey post-test was performed for normal data. Elsewise, we used Friedman test with Dunn's post-test.

In *Ex Vivo* pig 6 experiment, plasma sample at timepoint 3h was missing completely at random. Therefore, plasma values of pig 6 (1h and 9h ischemia) were excluded when Friedman test was utilized.

For tissue immunofluorescence comparison, we employed the non-parametric Kruskal-Wallis test to compare *Ex Vivo* 1h vs 9h ischemia limbs. In the *In Vivo* group, EP tissue signal was compared to the respective BL signal, using Mann-Whitney test.

Data of from plasma measurements are presented as scatter plot representing individual experiments with a line indicating the mean value. Similarly, data obtained from immunostaining are presented as floating bars spanning the minimum and maximum values, and mean represented by the middle line.

4 Results

4.1 Clinical overview

Throughout each experiment, several parameters were observed to monitor the status of the pig and the perfusion machine, and intervene according to a preset protocol. We aimed at a 12h of limb perfusion following ischemia time. All limbs exposed to 1h ischemia were perfusion for 12h ±0 unlike the 9h ischemia limbs. In *Ex Vivo* model, 9h ischemia limbs had a substantially shorter duration of perfusion (mean= 8.6h ± 3) with one limb lasting 12h, two limbs lasting 11h, another one lasting 7h and two limbs lasting less than 6h (5.40h). Comparably, 9h ischemia limbs in *In Vivo* model sustained longer perfusion time (mean= 9.8h ± 3.8) with only one limb reaching endpoint after 5.4h of perfusion (figure 5a). Amputated limbs were weighed immediately after amputation and again at endpoint, and ratio was calculated as an indication of limb edema. Limbs of 9h ischemia of both *Ex Vivo* and *In Vivo* groups had a substantial weight gain at endpoint –more evidently in *In Vivo* group- with an average ratio of 1.23 ± 0.05 and 1.37 ± 0.07, respectively. Comparatively, 1h ischmia limbs of both groups exhibited less to no difference in weight ratio with an average increase of 10% ± 3% in *Ex Vivo* and 12% ± 7% in *In Vivo* (figure 5b). However, wet/dry ratio analysis showed a substantial difference, yet marginal, only between the 9h and 1h ischemia limbs of the *In Vivo* group, mainly owing to the high ratio observed in pig 1 (figure 5c).

Measurement of arterial blood lactate in *Ex Vivo* limbs showed a rising trend in 1h ischemia limbs, however a significant ($P<0.0001$) *increase* in the 9h ischemia at endpoint (figure 5d). The observed increase of lactate levels in the circulating blood is due to its accumulation with no further clearance. Furthermore, perfused limbs of all groups had a comparable skin temperature at endpoint. A rising trend was observed among 9h ischemia limbs of both groups with lower temperature recorded at the beginning of perfusion (figure 5e & 5f).
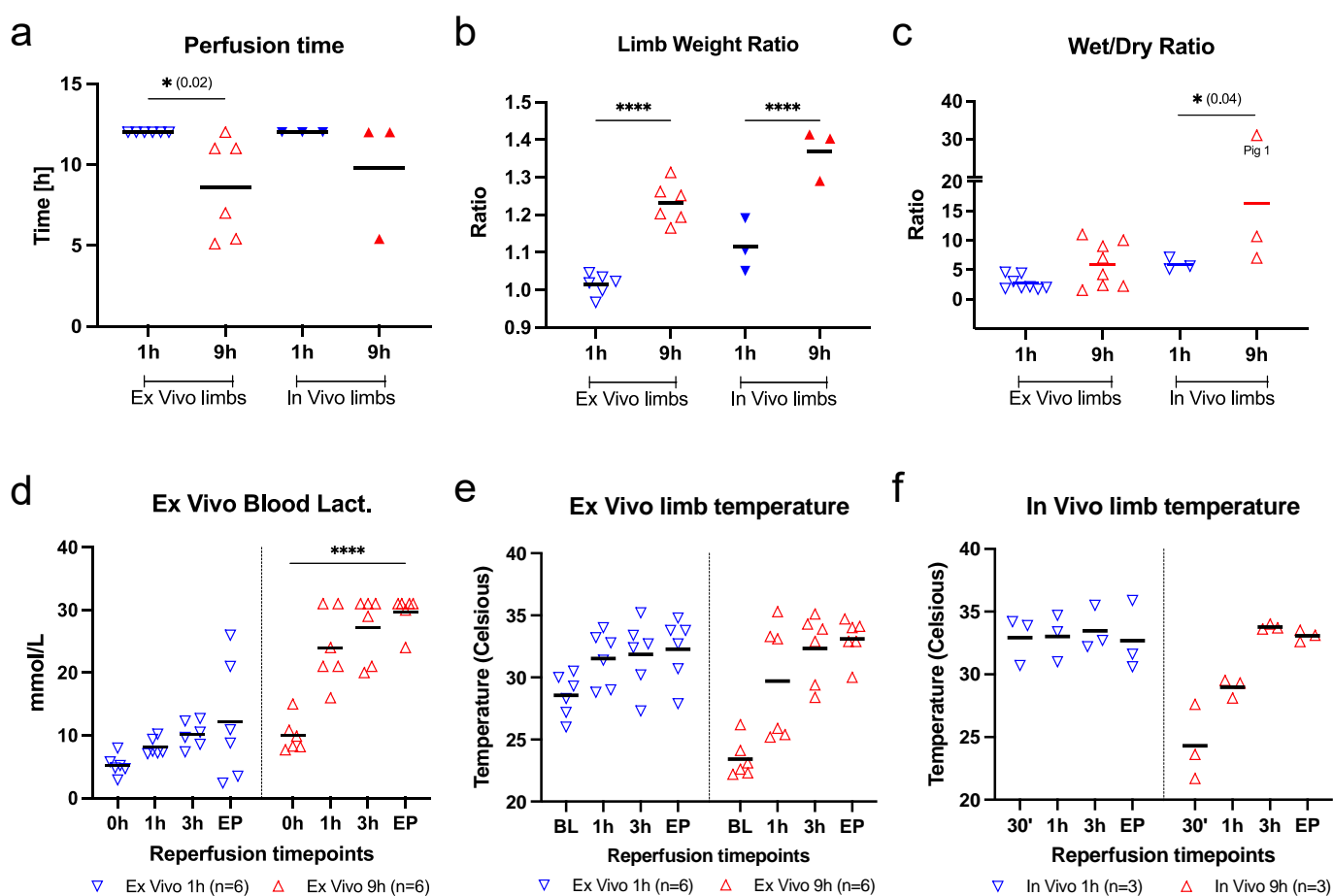
Figure 5 Clinical observations during *Ex Vivo* and *In Vivo reperfusion* experiments.
(a) Duration of perfusion of *Ex Vivo* (heart-lung machine) and *In Vivo* (replantation) limbs until reaching the endpoint. (b) Limb weight ratio defined as the limb weight at baseline before ischemia divided by the limb weight at the endpoint of perfusion. (c) Ten muscle punch biopsies were collected at endpoint and weight ratio was calculated before and after drying for 40 hr at 80°C in the oven. Measurements of blood lactate across *Ex Vivo* limbs (d) and carpal temperature of *Ex Vivo* (e) and *In Vivo* (f) limbs. Statistical analysis with paired *t*-test (d) and unpaired (a, b, d). **** $P < 0.000$.

4.2 Muscle tissue damage

A porcine-specific commercial ELISA kit was used to detect CKMM plasma levels across different timepoints of the experiment. Analysis of CKMM concentration in *Ex Vivo* 1h ischemia limbs (figure 6a) showed comparable values from BL until 3h of perfusion followed by a substantial rise at endpoint ($P= 0.01$ compared to 1h, $P= 0.002$ compared to 3h). In 9h ischemia limbs (figure 6a), a marginal increase of CKMM levels was observed at 3h of perfusion ($P= 0.08$) and reaching a significant level at endpoint compared to 1h perfusion ($P= 0.02$), and BL ($P= 0.002$). Comparatively, *Ex Vivo* 9h ischemia limbs had significantly higher plasma CKMM concentration compared to 1h ischemia ($P= 0.01$), however no difference was

observed at endpoint (figure6). In contrast, in *In Vivo* group (figure 6b), plasma CKMM levels were comparable in 1h ischemia limbs and a rising trend was observed among 9h ischemia limbs at endpoint compared to BL (P=0.05).

To observe the structural muscle damage at the endpoint of perfusion, we used an antibody against dystrophin –a cytoskeleton protein in skeletal muscle– for immunostaining to compare frozen cross-sections of BL and endpoint muscle samples. At baseline (figure 6), muscle fibers are arranged in hexagonal structures with intact endomysium. In 1h ischemia limbs *In Vivo* group we observed a similar structural integrity however, *Ex Vivo* 1h ischemia limbs exhibited a mild decomposition and displacement of muscle fibers. In contrast, severe damage was observed in 9h ischemia limbs of both groups as well as large displacement of muscle fibers as a sign of edema (figure 6).
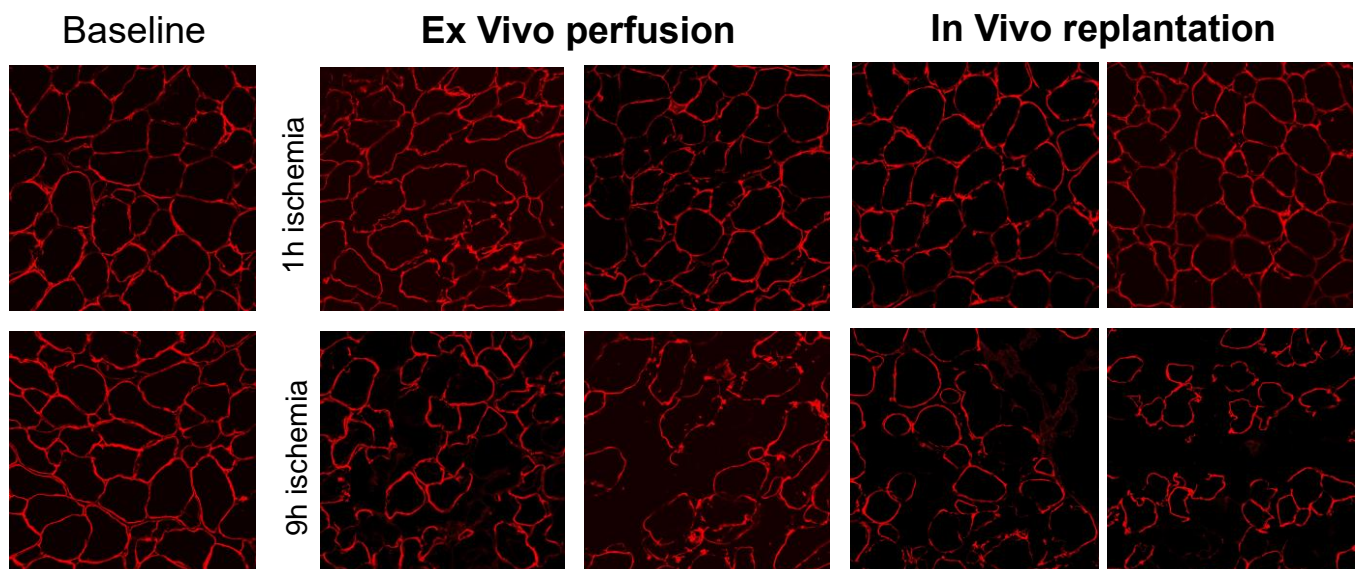
Figure 6 Evaluation of muscle injury in 1h and 9h ischemia limbs of both *Ex Vivo* and *In Vivo* limbs.

Muscle injury was evaluated by ELISA –plasma levels of Creatinine Kinase-MM (CKMM) across different timepoints– and tissue immunostaining for dystrophin (red) as a marker of muscle fibers. Muscle tissue samples were obtained at baseline and endpoint of reperfusion in all groups. Data for individual experiments are presented as scatter plot with a line indicating the mean (a, b). Images were acquired at 20x magnification and two representative images of muscle structure are shown for each group. Statistical analysis to compare timepoint differences between groups (# tagged) using Krukal-Wallis test, and within-group using Friedman test. * / # P <0.05, ** P <0.01.

4.3   Endothelial cell activation

Activation of endothelial cells induces upregulation and expression of surface adhesion molecules. Induction of E-selectin expression was analyzed across all limbs in both tissue – BL and EP- and serum at BL and 1h, 3h, EP of perfusion time, using a commercial porcine-specific ELISA kit. Analysis of soluble E-selectin in serum showed no significant differences in concentration at all timepoints across limbs of all groups. This indicates no shedding of E-selectin was observed.
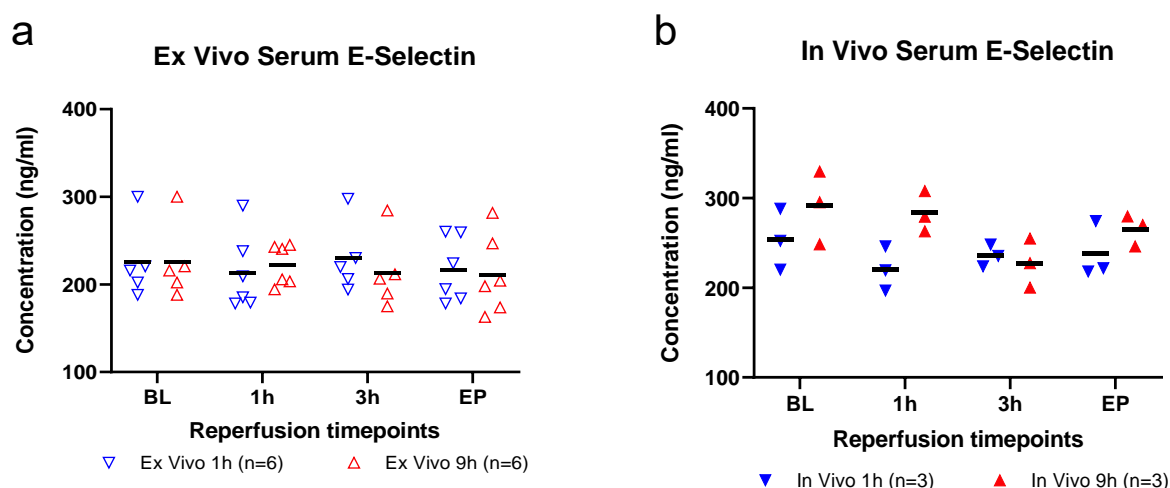
Figure 7 Measurement of soluble E-selectin in serum of *Ex Vivo* and *In Vivo* limbs. Soluble form of E-selecting was measured in *Ex Vivo* (a) and *In Vivo* (b) serum samples at BL, 1h, 3h and EP of perfusion using a commercially available porcine-specific ELISA. Data are represented as individual experiments with a middle-line indicating mean.

In contrast, immunostaining of E-selectin in tissue (figure 8) has revealed a substantial difference among groups. The mean fluorescence area of E-selectin signal was significantly higher in muscle tissue of 1h ischemia limbs compared to 9h ischemia limbs in *Ex Vivo* group ($P= 0.004$ – figure 8a). Comparably in *In Vivo* group, a higher signal was observed in 1h ($P= 0.04$) and 9h ischemia limbs compared to their baseline (figure 8b). Furthermore, *Ex Vivo* 9h ischemia limbs had a sizable signal compared to *In Vivo* BL ($P= 0.04$). This observation indicates an increased expression of E-selectin at endpoint of perfusion in both 1h and 9h ischemia limbs, however, more evident in 1h ischemia limbs.
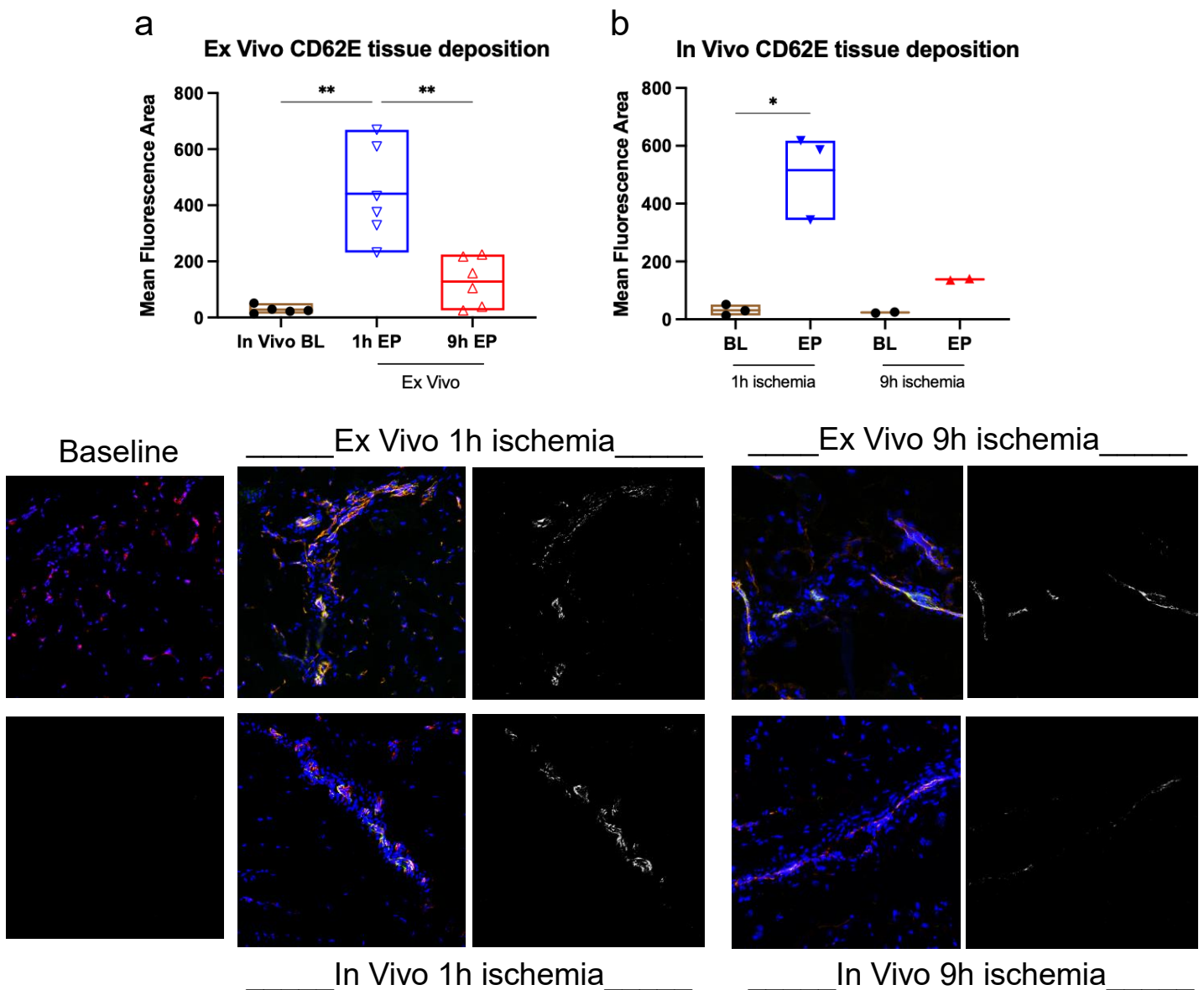
Figure 8 <u>Immunostaining of E-selectin expression in muscle tissue across *Ex Vivo* and *In Vivo* limbs.</u>

Stronger E-selectin (CD62E) signal was acquired in muscle tissue of 1h ischemia compared to 9h ischemia limbs of both groups. Muscle tissue were sectioned and immunostained for DAPI (blue), CD31 (red) and CD62E (green). Images were acquired at 20x magnification. A representative image for each group is displayed in color and in black & white for CD62E. Signal quantification was performed using imageJ. Statistical comparison was conducted using Brown-Forsythe test for *Ex Vivo* groups (a) and unpaired t-test for *In Vivo* groups (b). Data represented as individual values with middle line indicating mean value. *=P <0.05, **=P <0.01.

Furthermore, we looked at the differences in CD31 expression –also known as platelet endothelial cellular adhesion molecule-1 (PECAM-1)- in muscle tissue of all groups at baseline and endpoint (figure 9). There was no notable difference in CD31 immunofluorescence signal across all limbs. In *Ex Vivo* group (figure 9a), CD31 signal at endpoint was comparably less in the 9h ischemia limbs compared to 1h ischemia limbs. In addition, in *In Vivo* group (figure 9b), we observed a similar signal at endpoint in muscle tissue of both 9h and 1h ischemia limbs, however relatively less than the BL signal of the latter group.
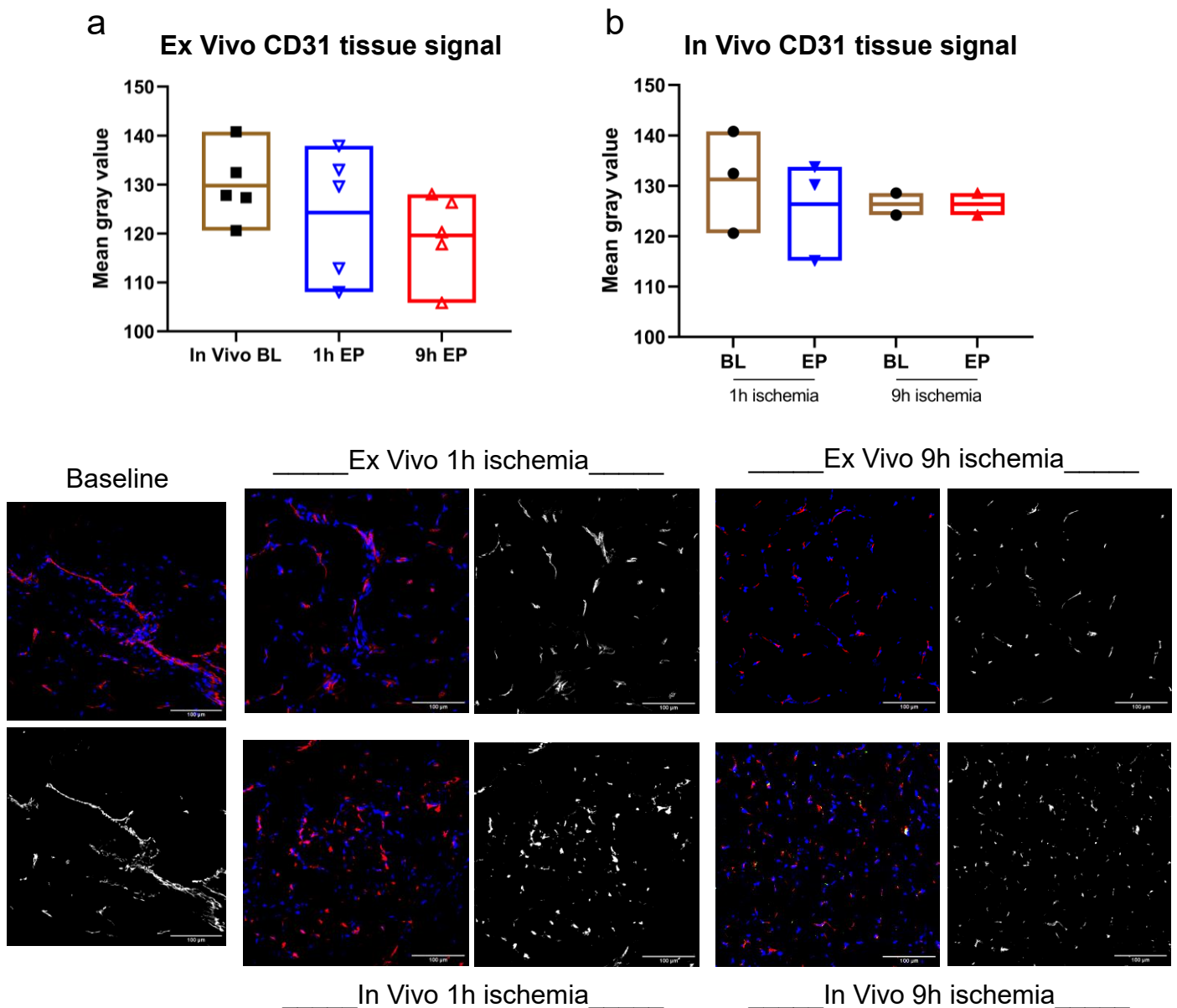

Figure 9 Immunostaining of CD31 expression in muscle tissue across *Ex Vivo* and *In Vivo* limbs.
Endothelial cell marker CD31 (PECAM-1) signal was acquired in muscle tissue of 1h ischemia compared to 9h ischemia limbs of both groups. Muscle tissue were sectioned and immunostained for DAPI (blue), CD31 (red). Images were acquired at 20x magnification. A representative image for each group is displayed in color and in black & white for CD31. Signal quantification was performed using imageJ. No significant difference observed across groups besides a relatively weaker signal in 9h compared to 1h ischemia of *Ex Vivo* group.

4.4   Growth factors expression

Growth factors among other cytokines were analyzed using an immunoplex multiplex assay as described in the methods section. This included vascular endothelial growth factor (VEGF), platelets derived growth factor (PDGF) and basic fibroblasts growth factor (bFGF). To compare plasma levels between groups, we used observed concentration for VEGF and bFGF, and values of raw fluorescence intensity for PDGF. In *Ex Vivo* 9h ischemia limbs (figure 10a-c), all growth factors demonstrated a rising pattern from BL values reaching a significant level at endpoint in both VEGF (P= 0.004) and PDGF (P= 0.03), and only comparable levels in bFGF. Likewise in 1h ischemia limbs and compared to BL, higher levels were observed at endpoint for VEGF (P= 0.02, compared to BL) and PDGF (P= 0.04, compared to 1h and 3h). Concentration of bFGF at endpoint was comparable to BL with a substantial difference seen when compared to 1h and 3h timepoints. A similar pattern was observed in PDGF. Additionally, there was a general trend of elevated plasma levels -across perfusion time- among the 9h ischemia limbs compared to 1h ischemia limbs, however, not significantly different.

Across *In Vivo* limbs (figure 10d-f), both VEGF and bFGF were significantly elevated at endpoint of perfusion compared to BL in 9h ischemia limbs, P= 0.009 and P= 0.03, respectively. As well, PDGF values were comparably higher at endpoint. In contrast, 1h ischemia limbs showed a marginal increase in VEGF at endpoint (P= 0.06). Moreover, no notable difference was detected between 1h and 9h ischemia limbs during perfusion.
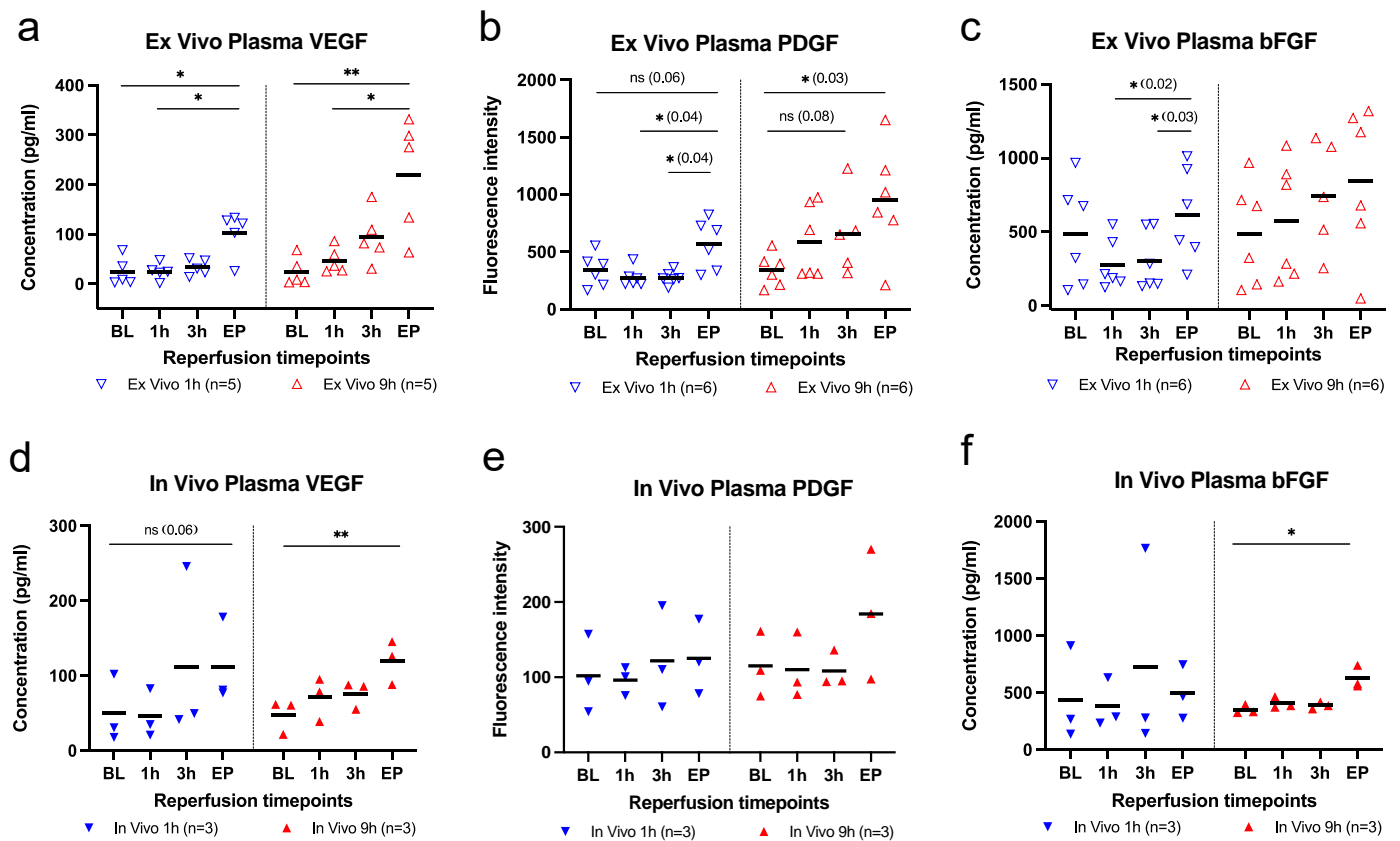
Figure 10 Analysis of growth factors across *Ex Vivo* and *In Vivo* limbs.

Plasma samples were analyzed using 11-Plex for VEGF, PDGF and bFGF. Statistical analysis to compare timepoint differences within group using Friedman test (a, c, d-f) and repeated measures ANOVA (b). Data of individual experiments represented as scatterplot and mean indicated by the line. VEGF, Vascular Endothelial Growth Factor; PDGF, Platelets Derived Growth Factor; bFGF, basic Fibroblasts Growth Factor. * $P < 0.05$, ** $P < 0.01$.
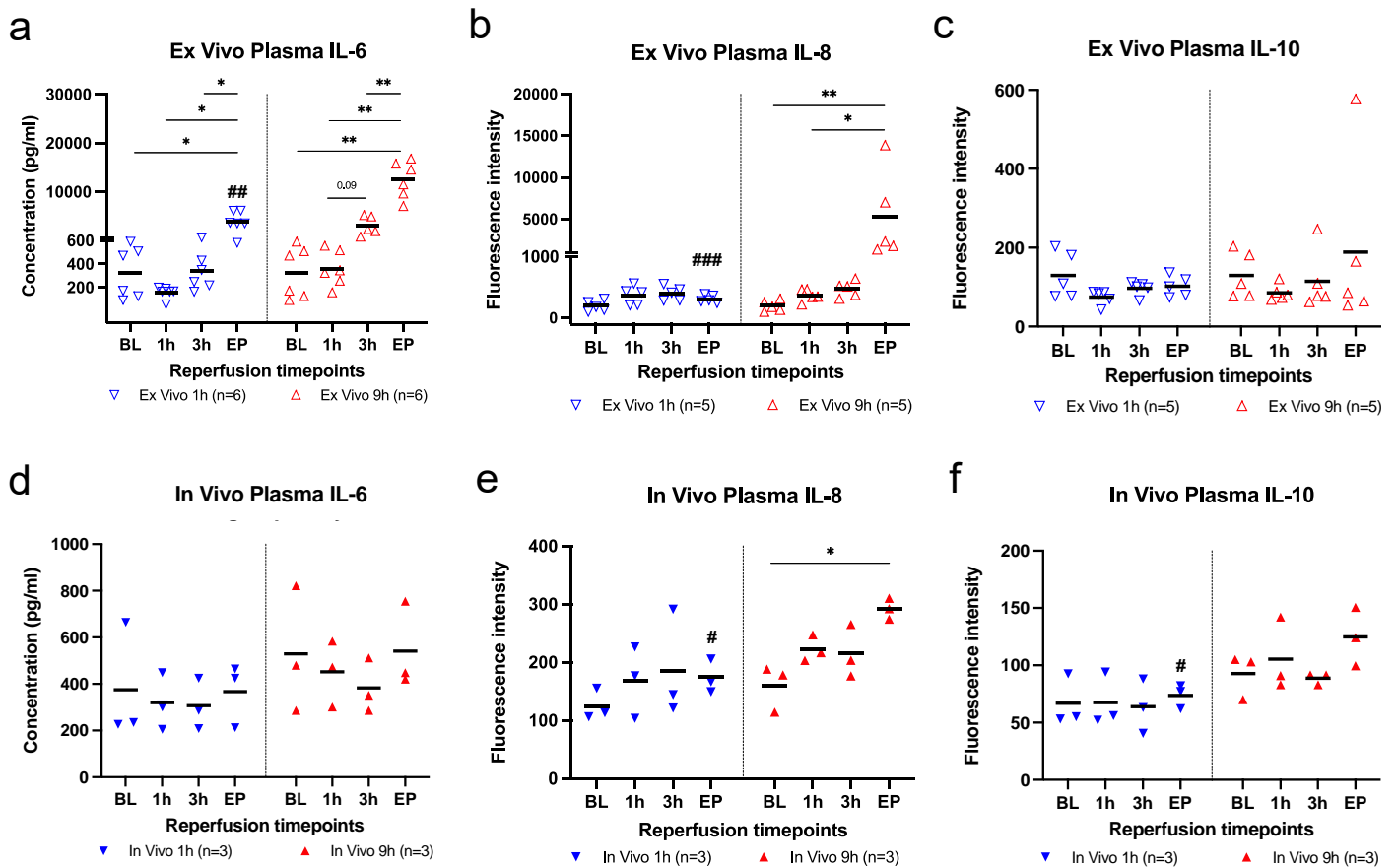
4.5 <u>Markers of inflammation (pro/anti) in plasma</u>

In order to assess the status of inflammation associated with IRI, we looked at the levels of different cytokines in plasma and examined muscle tissue samples for immune cells' infiltration. Pro-inflammatory cytokines including IL-6, IL-8 and TNF-alpha, anti-inflammatory cytokine IL-10 and Monocytes chemoattractant protein-1 (MCP-1) were evaluated as part of the 11-plex multiplex immunoassay.

Among *Ex Vivo* group (figure 11a-c), 9h ischemia limbs showed a steep rise of IL-6 and IL8, reaching a significantly higher level compared to BL ($P=$ 0.002 and $P=$ 0.004, respectively), as well compared to the EP of 1h ischemia limbs ($P<$ 0.001 and $P=$ 0.004, respectively). We also observed a sizeable increase of IL-6 concentrations at EP of 1h ischemia limbs compared to BL ($P=$ 0.03), however IL-8 levels remained unchanged across perfusion time.

Plasma levels of TNF-alpha had a notable increase after 1h of perfusion in both 1h and 9h ischemia limbs followed by a downtrend. The increase in 1h ischemia limbs was significant compared to BL ($P=$ 0.01). In 9h ischemia limbs, TNF-alpha (figure 12a, 12b) was marginally higher at 1h perfusion compared to baseline however levels were substantially higher compared to EP ($P=$ 0.009). Furthermore, plasma levels of the anti-inflammatory cytokine IL-10 demonstrated no evident change in both 1h and 9h ischemia limbs across perfusion time.

In comparison with the Ex Vivo group, a lesser inflammatory reaction was observed in among the In Vivo limbs (figure 11d-f). In 9h ischemia limbs, we observed a significant rise of IL-8 levels at the EP compared to BL (P= 0.01) as well to the EP of 1h ischemia limbs (P= 0.04). Likewise, a similar trend was detected in TNF-alpha measurements (figure 12a,12b) where plasma level at EP of 9h ischemia limbs was evidently higher compared to BL (P= 0.02), and to the EP of 1h ischemia limbs (P= 0.049). In addition, a general uptrend of IL-10 plasma levels was noted reaching a substantially higher level at EP compared to EP of 1h ischemia limbs (P= 0.02). Therefore, indicating a counter-regulatory status to inflammation associated with IRI damage. Comparably, measurements of IL-6, IL-8, IL-10 and TNF-alpha had no significant differences during perfusion in 1h ischemia limbs.

Figure 11 <u>Analysis of pro & anti-inflammatory markers across *Ex Vivo* and *In Vivo* limbs.</u>

Interleukin-6 (a, d), Interleukin-8 (b, e) and Interleukin-10 (c, f) were analyzed in plasma using 11-Plex multiplex immunoassay. Values of individual experiments presented as scatter plot with a line indicating the mean. Statistical analysis to compare timepoint differences between groups (# tagged) using Brown-Forsythe test (a) and Krukal-Wallis test (b, e, f), and within-group using repeated-measures ANOVA (a) and Friedman test (b,e). */# P <0.05, **/## P <0.01, ***/### P <0.001.
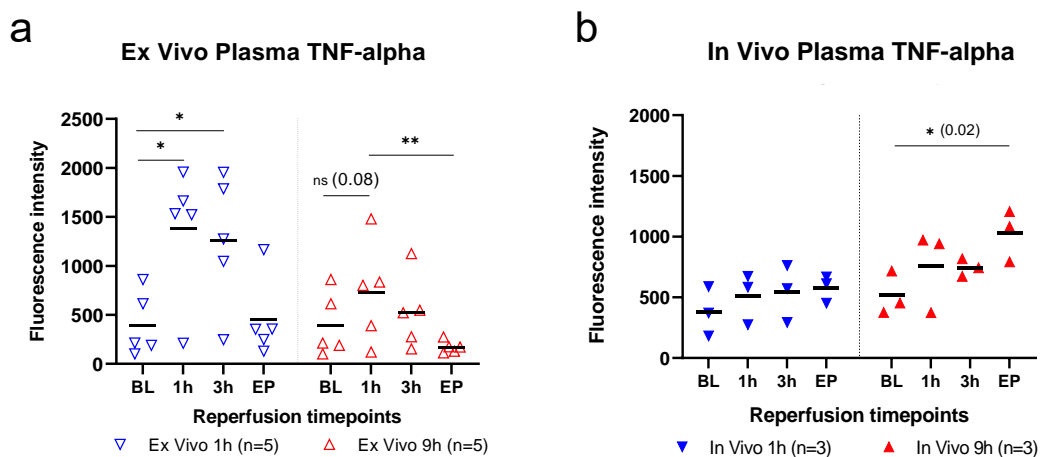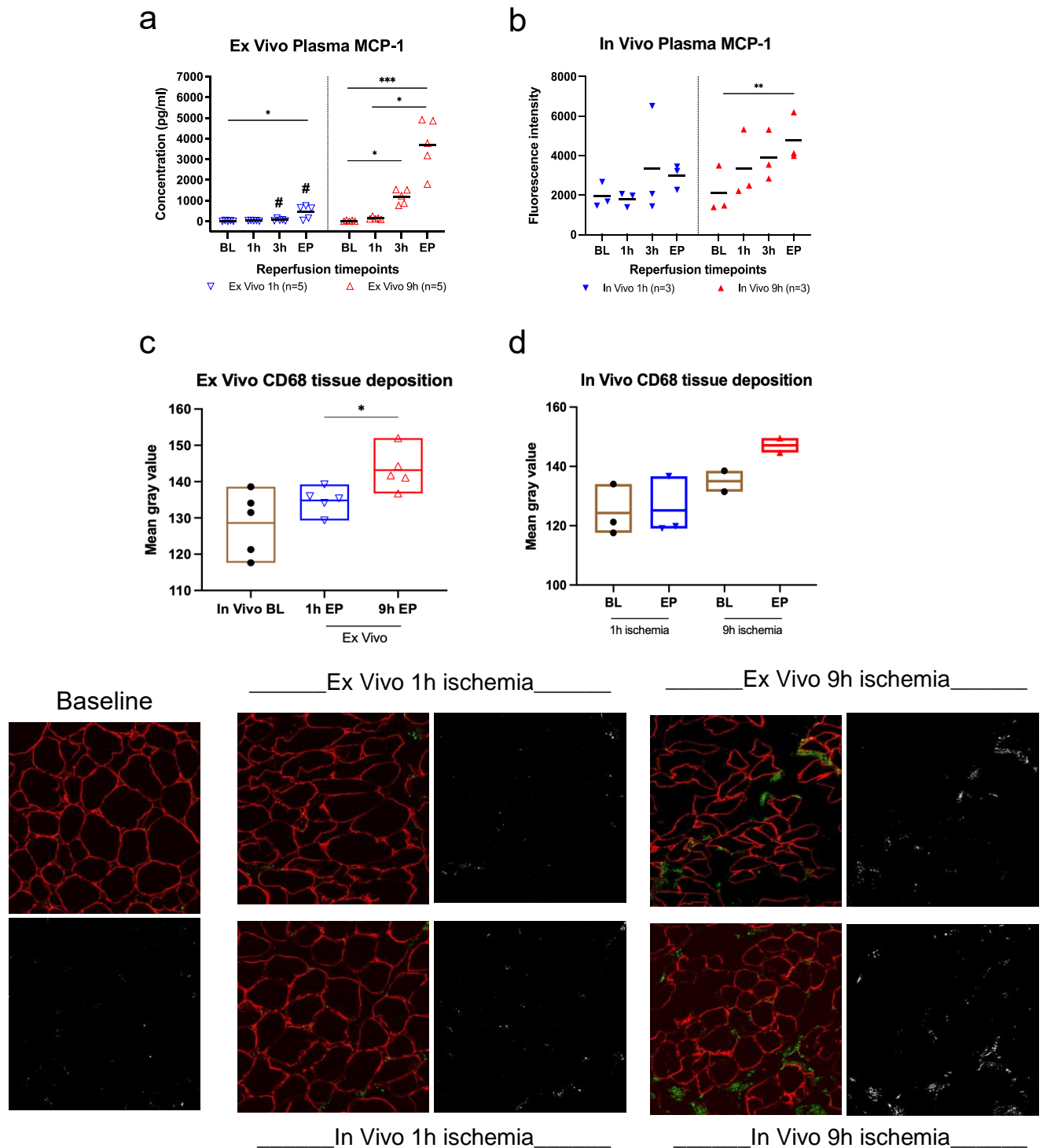

Figure 12 <u>Analysis of TNF-alpha in plasma across *Ex Vivo* and *In Vivo* limbs.</u>

Plasma levels of TNF-alpha were analyzed as part of the 11-Plex multiplex immunoassay. Values of individual experiments presented as scatter plot with a line indicating the mean. Statistical analysis to compare timepoint differences within-group using Friedman test. * P <0.05, ** P <0.01.

4.6   Infiltration of immune cells

Muscle tissue from at BL and EP were immunostained against CD68 –a marker for monocytes lineage– in order to examine the extent of their infiltration by the endpoint of perfusion. Analysis of the acquired images has revealed a significantly higher signal in the 9h ischemia limbs of *Ex Vivo* group compared to 1h ischemia limbs (P= 0.02, figure 13c). Among the *In Vivo* group, a stronger signal compared to BL was observed in muscle tissue of the 9h ischemia limbs, yet not significant (figure 13d). In contrast, there was no measurable difference in the signal acquired across the 1h ischemia limbs of *Ex Vivo* and *In Vivo* groups however; a comparably higher signal was detected among limbs of the *Ex Vivo* group. These findings indicate a higher activity of phagogcytosis and IRI induced monocytes and macrophages recruitment.

Besides –and as part of the inflammation milieu, monocytes chemoattractant protein-1 (MCP-1) is expressed at the site of inflammation acting as a chemokine to recruit immune cells, namely monocytes. Analysis of MCP-1 in plasma of *Ex Vivo* limbs (figure 13a) revealed a sizeable increase of MCP-1 both in 1h and 9h ischemia limbs. In 9h ischemia limbs (figure13a), the rise was as early as 3h (P= 0.04) of perfusion and continued increasing until EP (P= 0.0007). In addition, plasma levels at 3h and EP were significantly higher in the 9h compared to 1h ischemia limbs (P= 0.01 and P= 0.045, respectively). The observed rise in 1h ischemia limbs was only evident at EP compared to BL levels (P= 0.04, figure 13a). Opposed to these findings, only the *In Vivo* 9h ischemia limbs had an evident rise of MCP-1 level at EP compared to BL (P= 0.004 , figure 13b), and no substantial differences were detected in the 1h ischemia limbs.

Figure 13 Analysis of monocyte's chemokine and muscle infiltration across *Ex Vivo* and *In Vivo* limbs.

Plasma levels of monocyte chemoattractant protein-1 (MCP-1) were analyzed as part of the 11-Plex multiplex immunoassay. Values of individual experiments presented as scatter plot with a line indicating the mean. Higher concentrations of MCP-1 in 9h ischemia limbs of both groups, as well, in 1h ischemia limbs of *Ex Vivo* group. Baseline and endpoint muscle were stained for dystrophin (red) and CD68 (green). Images were acquired at 20x magnification and representative images are shown as colored for dystrophin and CD68 (left image) and as black and white for CD68 alone (right image). Data presented for individual experiments as floating bars with mean indicated by the middle line. Strong signal was observed at endpoint of 9h ischemia limbs of both *Ex Vivo* and *In Vivo* groups. Immunofluorescence quantification was performed using ImageJ, and Kruskal-Wallis test was employed for statistical comparison (#: timepoint comparison between groups). */# *P < 0.05,* ** *P* <0.01, *** *P* <0.001.

4.7 Complement cascade components

Different components of the complement cascade system were analyzed both the soluble forms in plasma and the deposition in muscle tissue. Complement component 3a (C3a) was analyzed in plasma using a commercially available and porcine-specific ELISA kit.

In *Ex Vivo group,* plasma concentrations of C3a (figure 14a) in both 1h and 9h ischemia limbs showed a substantial drop at the 1h of perfusion followed by a rising trend until EP. Only at EP of 9h ischemia limbs, C3a levels were significantly higher compared to BL values ($P= 0.005$), In addition, concentrations of C3a were significantly higher at 3h and EP of the 9h compared to 1h ischemia limbs, $P= 0.046$ and $P= 0.002$, respectively.

Looking at C5a plasma concentrations (figure 14b), we observed a sizable increase after 1h of perfusion in both 1h and 9h ischemia limbs, yet significantly higher in the latter ($P= 0.03$), compared to BL ($P= 0.04$ and $P= 0.002$, respectively). This increase was followed by a substantial decrease at 3h timepoint ($P= 0.03$ and $P=0.009$, respectively) and trending downwards until EP. To note, C5a levels in 9h ischemia limbs were marginally higher at 3h of perfusion compared to BL values ($P= 0.047$),

In addition, analysis of the soluble membrane attack complex (sC5b-9) demonstrated an evident increase in concentration across perfusion time (figure 14c). This increase exhibited a substantial and stepwise increase at 1h ($P= 0.009$), 3h ($P= 0.009$) and EP ($P= 0.0009$) of perfusion, in the 9h ischemia limbs. However, a significant level was reached only at EP in the 1h ischemia limbs ($P= 0.002$). Moreover, limbs of 9h ischemia had significantly higher concentrations of sC5b-9 at 1h ($P= 0.009$), 3h ($P= 0.02$), and EP ($P= 0.009$) compared to levels of 1h ischemia limbs.

Using immunostaining, we looked at the deposition of natural IgM and complement component 3b-c (C3b-c) in muscle tissue at BL and EP. The detected immunofluorescence signal of IgM was comparable in 1h and 9h ischemia limbs (figure 15a). However, in comparison with the BL signal from *In Vivo* limbs, IgM signal in 9h ischemia limbs was marginally stronger ($P= 0.04$), and as well in the 1h ischemia limbs ($P= 0.05$). Furthermore, analysis of C3b-c immunofluorescence signal (figure 16a) indicated a substantially larger deposition in muscle tissue of 9h ischemia limbs compared to 1h ischemia ($P= 0.01$). These findings highlight the activation of complement cascade system, which was sizably stronger among the 9h ischemia limbs.
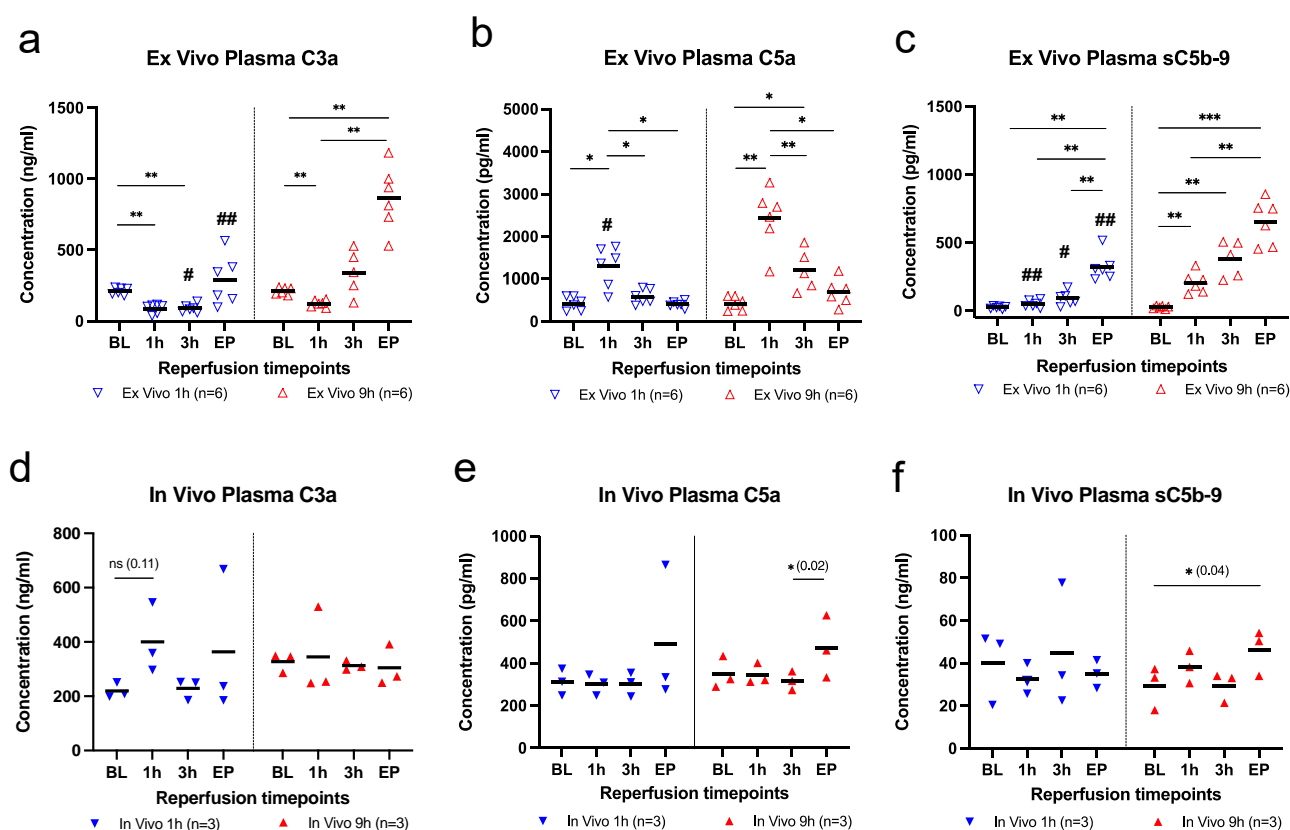
Figure 14 <u>Analysis of plasma complement components across *Ex Vivo* and *In Vivo* limbs</u>.
Different complement components were detected in plasma samples using ELISA (C3a) and 11-Plex multiplex assay (C5a, sC5b-9). Timepoint measurements of C3a (a, b), C5a (c, d) and sC5b-9 (e, f). Statistical analysis to compare timepoint differences between groups (# tagged) using Brown-Forsythe test (a) and within group using repeated-measures ANOVA (b, d, f). Data presented as scatter plot and mean indicated by the line. */# *P* < 0.05, **/# *P* <0.01, *** *P* <0.001. sC5b-9: soluble complex of complement components 5b, 6, 7, 8 and 9.

In contrast to the *Ex Vivo* group, complement cascade activation was less pronounced. In 9h ischemia limbs, C3a plasma levels showed no significant change during perfusion time (figure 14d). However, plasma concentration of both C5a and sC5b-9 (figure 14e-f) demonstrated a substantial increase at the endpoint of perfusion compared to BL (*P*= 0.02 and *P*= 0.04, respectively). In 1h ischemia limbs, C3a, C5a and sC5b-9 concentrations remained comparable during perfusion time. In addition, there was no significant difference detected between 1h and 9h ischemia limbs, throughout perfusion time, across all three complement-components. Furthermore, among 9h ischemia limbs, we observed an increased tissue deposition of both IgM (figure 15) and C3b-c (figure 16) in muscle at endpoint compared to baseline (*P*= 0.04 and *P*= 0.02, respectively). However, in 1h ischemia limbs, the obtained signal of IgM and C3b-c was only comparable with no substantial difference between EP and BL.
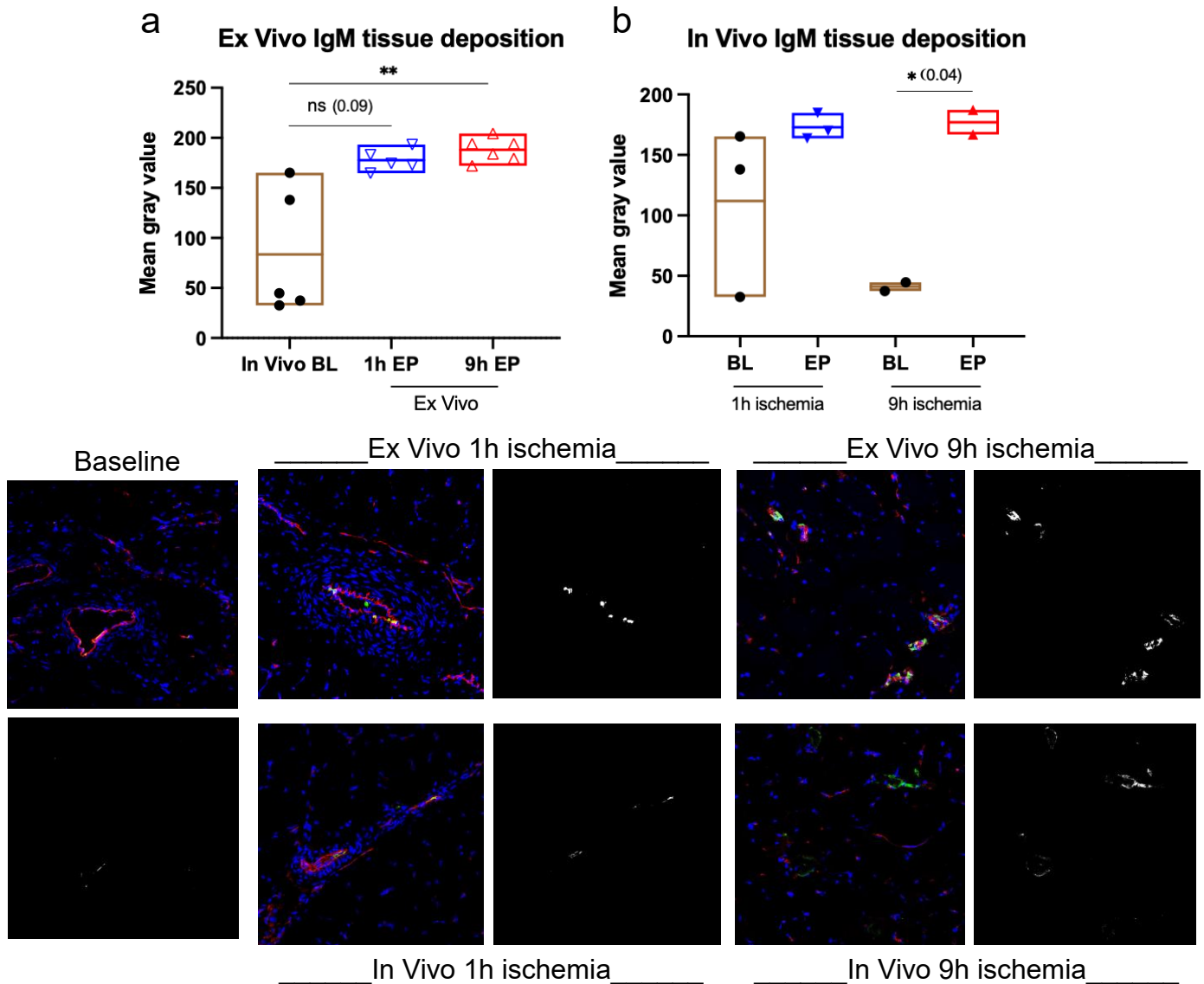
Figure 15 Immunostaining of IgM tissue deposition signal across *Ex Vivo* (A) and *In Vivo* (B) limbs.
Baseline and endpoint muscle were stained for DAPI (blue), CD31 (red) and IgM (green). Images were acquired at 20x magnification and representative images are shown as colored for IgM and CD31 (left image) and as black and white for IgM alone (right image). Data presented for individual experiments as floating bars with mean indicated by the middle line. Immunofluorescence quantification was performed using ImageJ. * $P < 0.05$, ** $P < 0.01$, computed by Kruskal-Wallis for *In Vivo* comparison and Brown-Forsythe for *Ex Vivo* comparison.

.
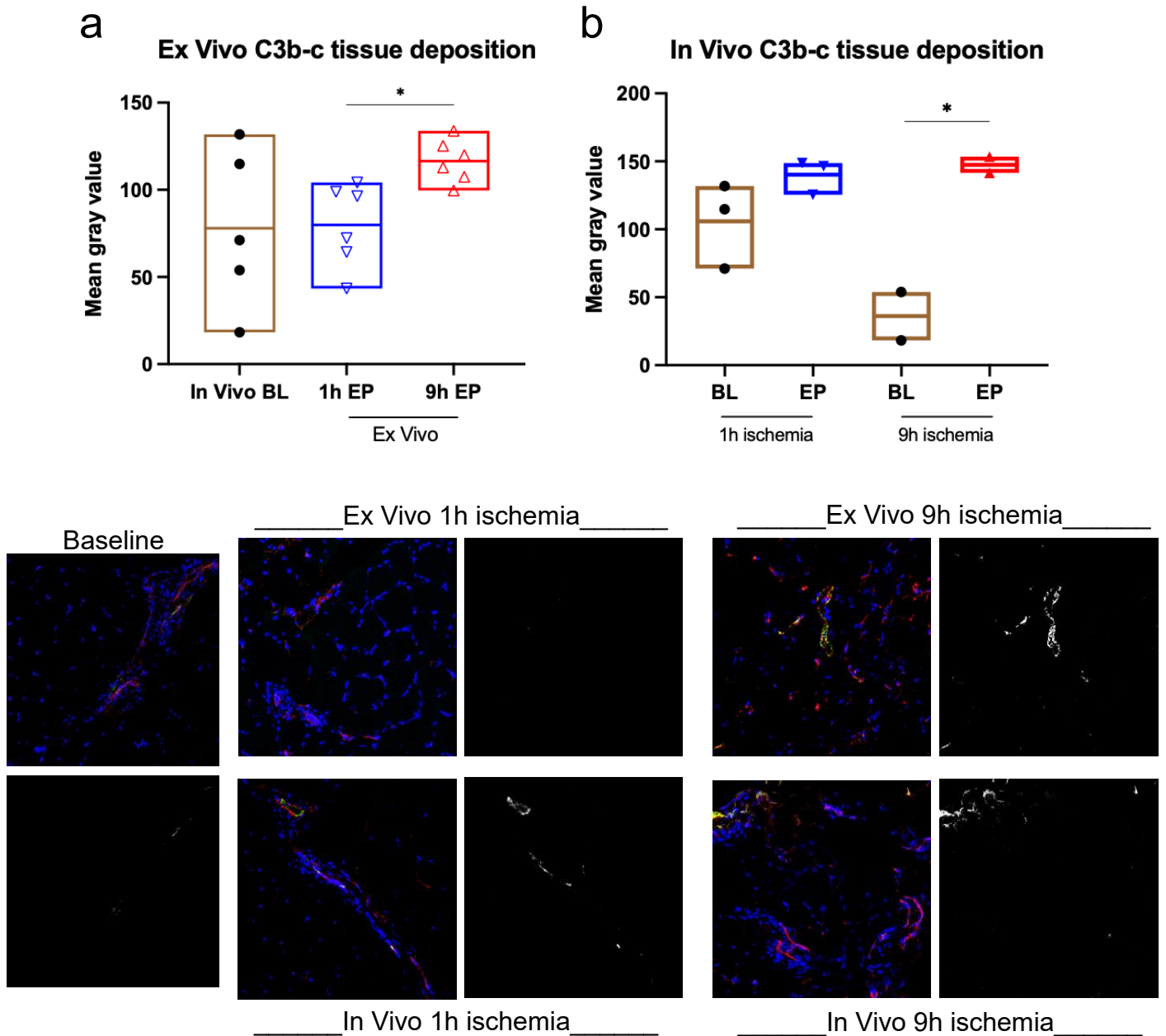
Figure 16. Immunostaining of C3b/c tissue deposition signal across *Ex Vivo* (A) and *In Vivo* (B) limbs.
Baseline and endpoint muscle were stained for DAPI (blue), CD31 (red) and C3b-c (green). Images were acquired at 20x magnification and representative images are shown as colored for IgM and CD31 (left image) and as black and white for C3b-c alone (right image). Stronger signal of C3b-c was observed in 9h ischemia limbs of both groups. Data presented for individual experiments as floating bars with mean indicated by the middle line. Immunofluorescence quantification was performed using ImageJ. *: *P < 0.05*, ** *P* <0.01, computed by Kruskal-Wallis for *In Vivo* comparison and Brown-Forsythe for *Ex Vivo* comparison.

4.8 <u>Thrombotic – Fibrinolytic systems</u>

4.8.1 Coagulation markers (vWF – TF – Fibrin)

In order to inspect the differences of coagulation activity in both groups, we looked at vWF and tissue factor (TF) levels in plasma, using a commercial and porcine-specific ELISA kits. In addition, we compared the deposition of fibrin(ogen) in muscle tissue at BL and EP across groups.

In *Ex Vivo* 9h ischemia limbs (figure 17a), plasma levels of TF had a substantial drop at 1h of perfusion ($P= 0.03$) and remained comparably at a similar level until endpoint ($P= 0.048$, compared to BL). However, *Ex Vivo* 1h ischemia limbs showed a significant increase at the 1h of perfusion ($P= 0.002$) followed by decrease in concentration reaching a substantial drop at endpoint ($P= 0.01$, compared to BL). In addition, TF plasma levels were notably higher at 1h and 3h timepoints in 1h compared to 9h ischemia limbs ($P= 0.0004$ and $P= 0.03$, respectively). Analysis of vWF in plasma (figure 17b) has shown a marginal drop in concentration after 1h of perfusion in both 9h and 1h ischemia limbs ($P= 0.07$ and $P= 0.05$, respectively), and decreasing significantly at 3h timepoint in the latter ($P= 0.02$). In 9h ischemia limbs, vWF levels started to rise at 3h and continued to increase until EP reaching significantly higher levels compared to 1h ischemia limbs ($P= 0.0004$ and $P= 0.002$,respectively).

In contrast to the *Ex Vivo* group, plasma concentrations of TF in *In Vivo* group (figure 17c) had no sizable differences in both 1h and 9h ischemia limbs across perfusion time. Tissue factor levels were similar in 1h ischemia limbs however; we observed a relative drop in concentration from 3h timepoint among the 9h ischemia limbs. Moreover, plasma levels of vWF (figure 17d) exhibited a rising pattern in both 1h and 9h ischemia limbs. The observed increase in 1h ischemia limbs continued until endpoint, yet with no substantial difference detected. In 9h ischemia limbs, vWF concentration was significantly higher at 3h of perfusion ($P= 0.01$, compared to BL) followed by a drop at endpoint, however remained relatively higher than BL level. In addition, 9h ischemia limbs had marginally higher levels of vWF at 1h timepoint compared to 1h ischemia limbs ($P= 0.04$)

In order to observe coagulation activity in muscle tissue, we used an antibody, which reacts against native fibrinogen as well to fragment D and E. We did not detect any significant differences in fibrinogen signal in muscle tissue between 1h and 9h ischemia limbs of both groups (figure 18). However, in *Ex Vivo* group, fibrinogen signal in tissue was comparably higher than the signal obtained in 9h ischemia limbs. In *In Vivo* group, 9h ischemia limbs had a similar signal at BL and EP, and 1h ischemia limbs showed a comparably weaker signal at EP from BL.
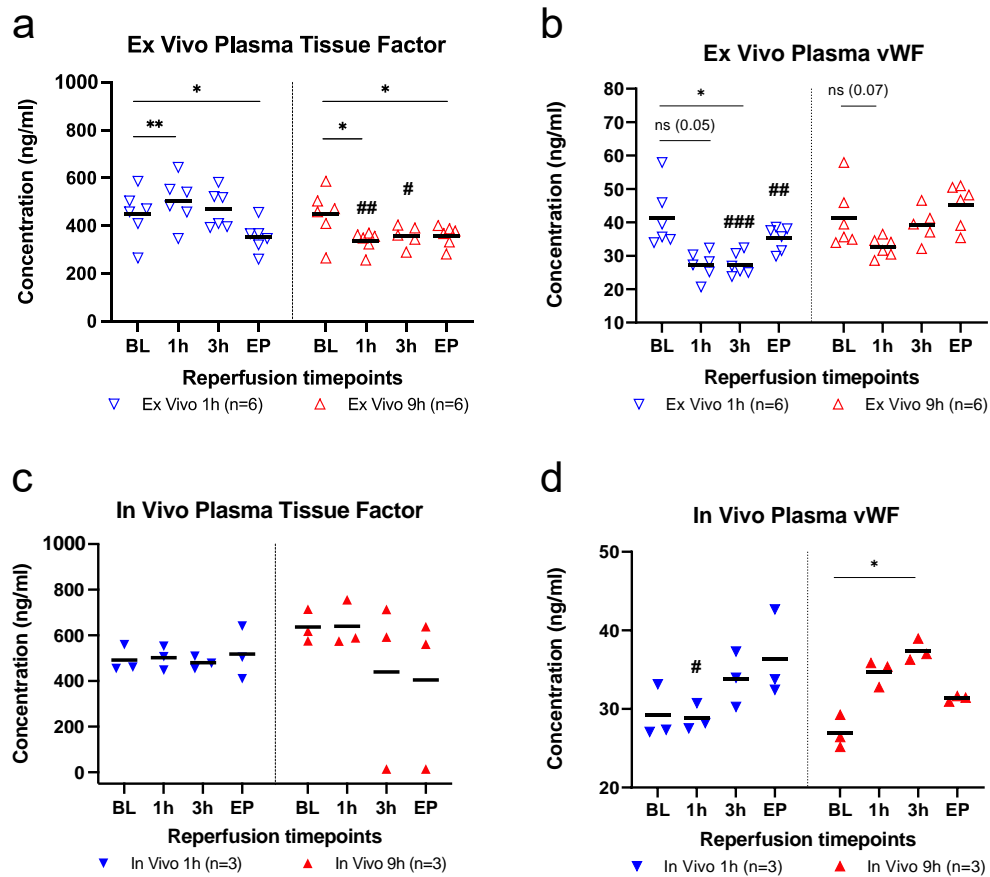
Figure 17 Analysis of coagulation activity in plasma across *Ex Vivo* and *In Vivo* limbs. Plasma measurements of tissue factor (TF) and von-willibrand factor (vWF) using commercial ELISA kits. Timepoint measurements of TF (a, c) and vWF (b, d). Statistical analysis to compare timepoint differences between groups (# tagged) using One-way ANOVA for *Ex Vivo* group and Kurskal-Wallis test for *In Vivo* group. Similarly, within group analysis using repeated-measures ANOVA and Friedman test. Data presented as scatter plot and mean indicated by the line. */# $P < 0.05$, **/## $P < 0.01$, ***/### $P < 0.001$
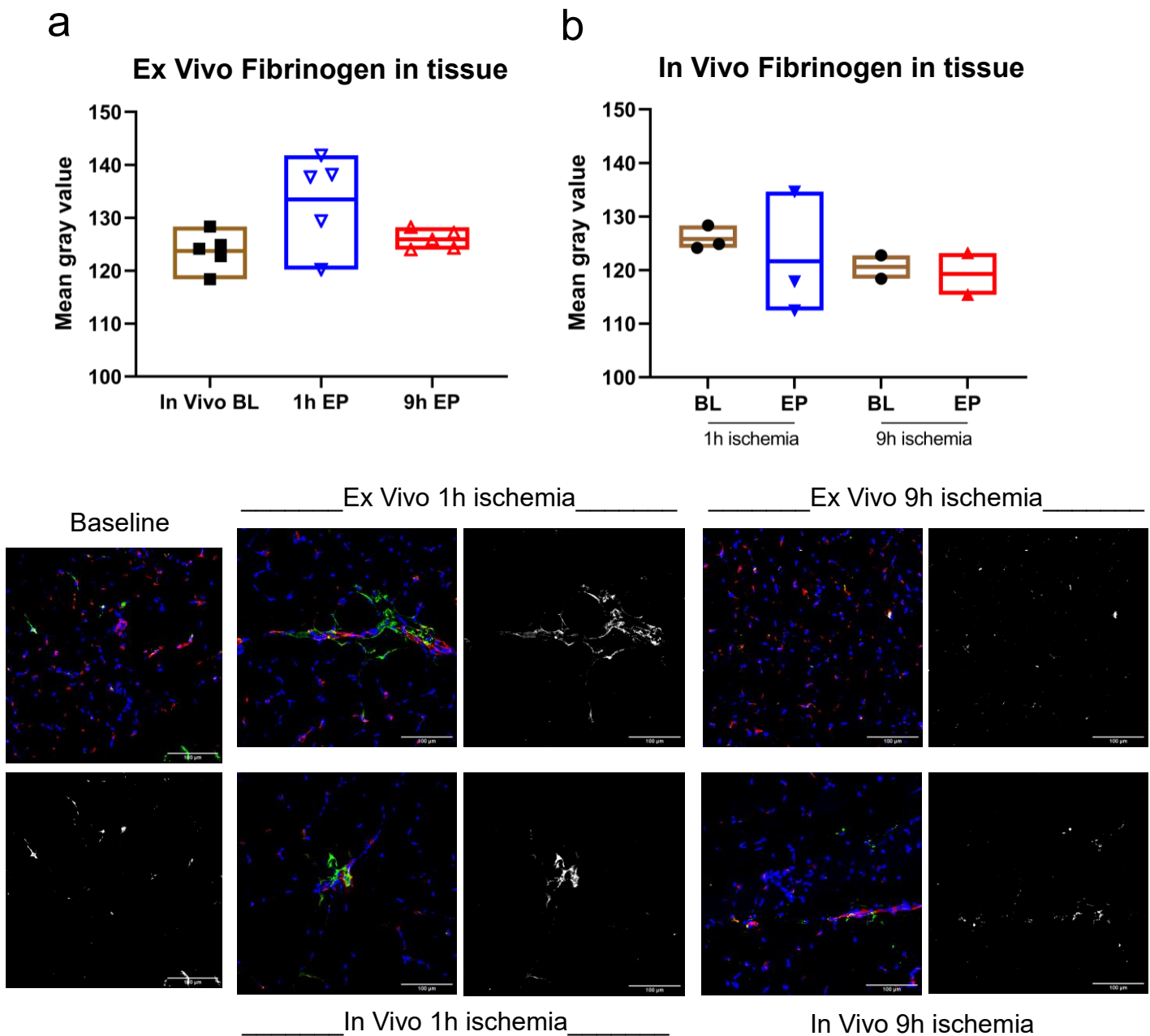
Figure 18 <u>Immunostaining of fibrinogen tissue deposition signal across *Ex Vivo* (A) and *In Vivo* (B) limbs</u>.
Baseline and endpoint muscle were stained for DAPI (blue), CD31 (red) and fibrinogen (green). Images were acquired at 20x magnification and representative images are shown as colored for IgM and CD31 (left image) and as black and white for IgM alone (right image). Data presented for individual experiments as floating bars with mean indicated by the middle line. Immunofluorescence quantification was performed using ImageJ. No significant differences detected in limbs of both groups.

4.8.2 Fibrinolytic activity markers (PAI-1/tPA complex – D-Dimer)

The activity of the plasma fibrinolytic system was evaluated by measuring the concentrations of both D-Dimer and plasminogen activator inhibitor-1/tissue plasminogen activator (PAI-1/tPA) complex in plasma.

Among *Ex Vivo* limbs (figure 19a, b), plasma concentrations of PAI-1/tPA showed a sizable increase from BL values throughout perfusion time. In 1h ischemia limbs, PAI-1/tPA concentration at EP was substantially higher compared to BL and 1h values ($P= 0.03$ and $P= 0.006$, respectively). In 9h ischemia limbs, a significant increase of PAI-1/tPA was detected as early as 3h ($P= 0.04$) of perfusion and kept rising substantially until EP ($P= 0.007$, compared to BL). In addition, plasma levels were higher at 1h ($P= 0.07$) and 3h ($P= 0.04$) timepoints in the 9h compared to 1h ischemia limbs. Furthermore, D-Dimer levels in plasma had no significant difference during perfusion time. However in 1h ischemia limbs, there was a comparable drop after 1h of perfusion followed by a rise in concentration reaching a substantial level at EP ($P= 0.02$, compared to 1h timepoint).

In contrast to *Ex Vivo* group, PAI-1/tPA in plasma of *In Vivo* 1h ischemia limbs (figure 19c) showed a similar rising pattern during perfusion time reaching a marginally significant level at EP ($P= 0.08$). However in 9h ischemia limbs, a significant rise was observed after 3h of perfusion ($P= 0.03$, compared to BL) followed by a comparable decrease with no substantial difference between both *In Vivo* groups. Moreover, plasma levels of D-Dimer (figure 19d) showed a relative drop at 1h timepoint among the 1h ischemia limbs ,and similar to the *Ex Vivo* group. In comparison, there was a marginal increase ($P= 0.07$) at 1h timepoint in the 9h ischemia limbs, which was substantially higher ($P= 0.04$) compared to 1h ischemia limbs.
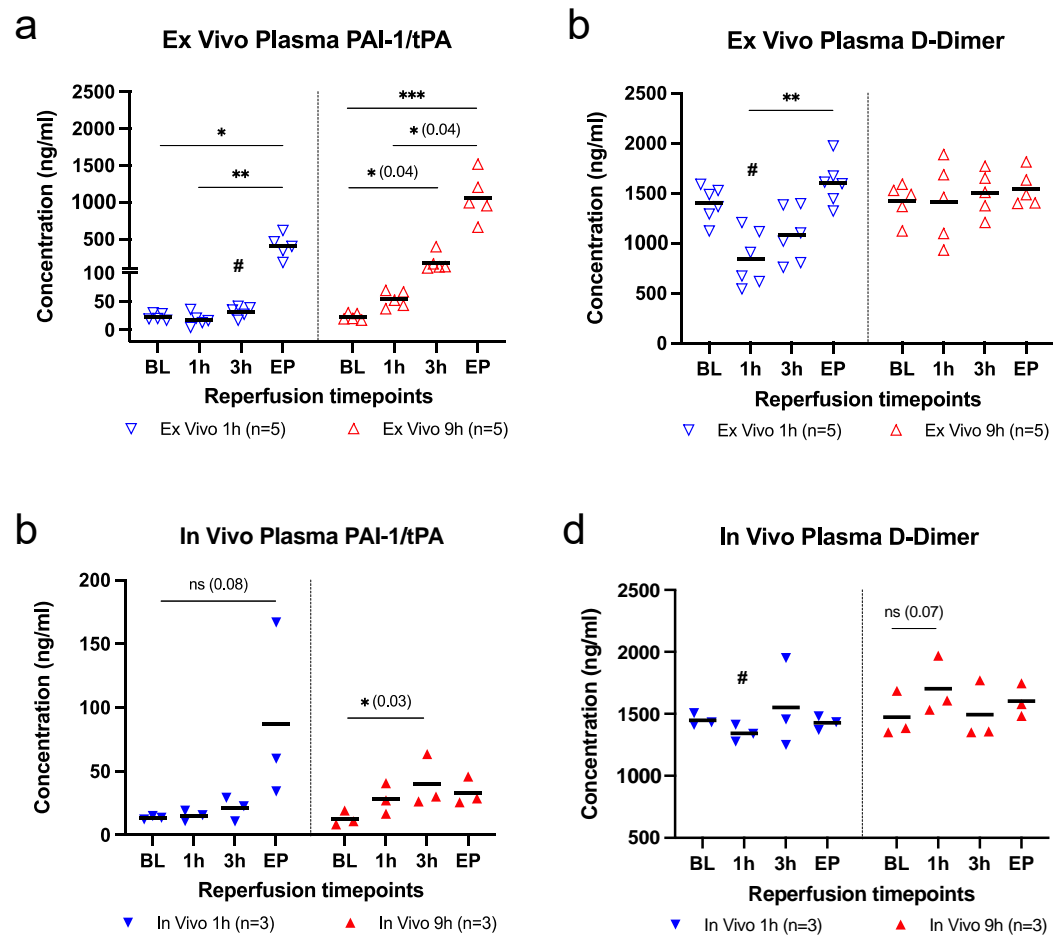
Figure 19. Analysis of Fibrinolytic markers in plasma across *Ex Vivo* and *In Vivo* limbs.
Plasma measurements of PAI-1/tPA complex and D-Dimer using commercial ELISA kits. Timepoint measurements for *Ex Vivo* group (a-d) and *In Vivo* group (e-h). Statistical analysis to compare between groups (# tagged) using - Kurskal-Wallis test. As well, within group analysis using Friedman test. Data presented as scatter plot and mean indicated by the line. */# *P* < 0.05, ** *P* <0.01, *** *P* <0.001.

5 Discussion

Our preliminary findings suggest the feasibility of our large animal model for *Ex Vivo* and *In Vivo* limb reperfusion injury following a prolonged ischemia time. Hereby, our early results detected the aggravated –and comparable– insult induced by limb reperfusion in both models, as shown by the trajectory of different cytokines, growth factors, EC activation markers and complement cascade activity –as well by tissue immunostaining. Notably, IRI was more pronounced among *Ex Vivo* reperfused limbs in contrast to replanted limbs. This could be explained by the sterile inflammatory environment induced by machine tubing system[38].

Across both reperfusion settings, 9h ischemic *Ex Vivo* limbs had a shorter perfusion time with only one limb reaching 12h of perfusion. Evident edema was detected in 9h ischemia limbs both by the relative gain of weight post reperfusion and by the widely-displaced muscle fibers observed by muscle tissue immunostaining. This was also indicated by the large increase of recorded compartmental pressure in replanted limbs. Edema formation is a result of vascular leakage following the disruption of EC junction –as a result of immune cell transmigration and loss of EC. Additionally, the plasma lactate build up in *Ex Vivo* setting is due to the absence of its utilization by the liver.

Creatine Kinases (CK) are a family of three iso-enzymes located intracellularly. Namely, CKMM –largely present in skeletal muscle, CKMB –exclusively in myocardial cells, and CKBB in brain tissue. Higher levels of circulating CK enzyme is an indication for tissue damage and cellular death. In our study, we evaluated plasma concentrations of CKMM as a marker of skeletal muscle damage [39], which exhibited a pronounced elevation among 9h ischemia limbs. Additionally, skeletal muscle injury was apparent in *Ex Vivo* 1h ischemia limbs after 6h of perfusion. In line with higher CKMM levels of 9h ischemia limbs, immunostaining of muscle tissue confirmed a pronounced structural damage –and similarly mild structural decomposition in 1h *Ex Vivo* limbs.

Resident macrophages play a vital role in maintaining homeostasis and promoting regeneration of skeletal muscles [40] –yet, a double-edged sword owing to their ability in prompting and limiting resolution following muscle injury [41]. Our tissue immunostaining showed stronger signal in *Ex Vivo* and *In Vivo* 9h ischemia limbs in line with other muscle damage markers. Furthermore, Monocytes Chemoattractant Protein-1 (MCP-1) was analyzed as part of the 11-Plex assay –which showed significant elevation across limbs of all groups except for the *In Vivo* 1h ischemia limbs. Notably, the observed increase was stronger among *Ex Vivo* limbs, and as fast as 3h of perfusion in the 9h ischemia limbs. In skeletal muscle, the role of MCP-1 is involved in both inflammation and regeneration [42] with a protective role exhibited in a mice model of kidney IRI [43].

Following restoration of limb circulation, ECs are the first to interact with tissue debris of the ischemic limb. This –in addition to hypoxia– promote the activation of EC into a pro-inflammatory and anti-fibrinolytic phenotype through the transcription of NF-κB [44]. Besides its downstream pro-apoptotic role, it induces the secretion of interleukins, growth factors, adhesion molecules, and the expression of PAI-1 on EC surface.

Our porcine-specific 11-Plex assay [37] included the detection of plasma IL-6, IL-8 and IL-10 among other markers. Plasma levels IL-6 were significantly elevated in both *Ex Vivo* 1h and 9h ischemia limbs and remained unchanged across *In Vivo* limbs. Interleukin-6 is a potent inflammatory marker induced by Lipopolysaccharides and other cytokines including TNF-alpha –the latter produced by macrophages and monocytes [45]. Looking at TNF-alpha plasma levels showed a sharp rise after 1h of perfusion in *Ex Vivo* limbs and a measurable rise only at EP in *In Vivo* 9h ischemia limbs. Thereafter, this correlation could explain the unchanged IL-6 values in the latter.

Interleukin 8 is a chemokine encoded by CXCL8 gene and secreted by different cells including EC. It exerts a potent chemoattractant characteristic for neutrophils aiding in their recruitment and activation. Blockage of IL-8 by neutralizing monoclonal antibodies exhibited a great reduction of myocardial IRI in rabbits [46]. In IRI setting, IL-8 is mainly secreted following reperfusion [47]. In our study we observed a strong presence of IL-8 in plasma at EP of 9h ischemia limbs in both reperfusion settings. Additionally, only *In Vivo* 9h ischemia limbs we observed an increase of the anti-inflammatory IL-10, which could further explain the less pronounced inflammatory state of IRI in *In Vivo* reperfusion.

Other surface markers of EC activation are E-selectin (CD62E) [23] and Platelets Endothelial Cellular Adhesion Molecule-1 (PECAM-1 or CD31). CD31 is expressed not only on EC but also on platelets and leukocytes [48]. Upon cellular interaction, CD31 triggers a downstream inhibitory and protective signaling including for instance leukocytes detachment. Following leukocytes transmigration, cleavage of CD31 takes place to limit further cellular infiltration [48]. Prevention of CD31 cleavage has shown protective effects in a model of rat mesentric IRI [49]. We observed a comparably weaker tissue signal of CD31 in *Ex Vivo* 9h ischemia limbs compared to the signal of BL and 1h ischemia limbs, yet not significant. This suggests the cleavage phenomena of CD31 and comparable with our previous data [50]. However, across *In Vivo* limbs, CD31 signal showed no differences.

Analysis of E-selectin tissue expression indicated a prominent signal across 1h compared to 9h ischemia limbs of both models. Earlier study demonstrated that E-Selectin following its expression on EC gets internalized –not shed– and degraded by lysosomes [51]. This corresponds to the detected serum E-selectin values, which remained unchanged during perfusion time. The observed weaker signal across 9h ischemia limbs could be due to the extensive loss of EC induced by IRI. As shown in a rat model of IRI, expression of E-Selectin

was observed only during reperfusion –not during ischemia [52]. In a study of human abdominal aortic aneurism, E-Selectin expression was detected in quadriceps muscle as early as 30' after clamp release [53]. Therefore, it remains unknown whether an earlier tissue biopsy could be more representative.

Furthermore, the reduced fibrinolytic state of EC activation is mediated by the surface expression of PAI-1, which inactivates tPA forming PAI-1/tPA complex. We hereby analyzed plasma levels of PAI-1/tPA complex across all limbs. Our results further indicate the more pronounced EC activation state in the *Ex Vivo* setting compared to *In Vivo*. This is further supported by the unchanged D-dimer plasma levels across perfusion time and in line with our previous data [50].

Expression of growth factors –namely VEGF and PDGF– is induced by ischemia through the transcription of NF-κB, which promote vascular angiogenesis. Plasma levels of VEGF and PDGF demonstrated a similar response as seen by VEGF in 9h ischemia limbs of both settings, and PDGF in *Ex Vivo* 9h ischemia limbs.

Analysis of complement activity in both reperfusion settings demonstrated a stronger activation across *Ex Vivo* limbs compared to *In Vivo*. This is partially amplified by the machine tubing system as previously indicated [38]. Complement activation in IRI of skeletal muscle is induced by both classical –immunoglobulins deposition– and MBL pathway [34-35]. As part of our tissue biopsy analysis, we tested for the deposition of IgM and complement component 3b/c (C3b/c). The obtained tissue signal of IgM and C3b/c was significantly stronger in 9h ischemia limbs of both models. Other complement markers were analyzed as part of our 11-Plex assay including C3a, C5a and soluble membrane attack complex (sC5b-9). In *Ex Vivo* limbs, a significant increase was observed across 1h and 9h ischemia limbs at EP, and only after 1h of perfusion in reference to C5a. Complement activity in *In Vivo* limbs was relatively weaker as only C5a and sC5b-9 demonstrated a significant increase only at EP of 9h ischemia limbs. Several complement regulatory proteins play a role in modulating tissue injury and complement activation. These proteins include decay-accelerating factor (DAF), complement receptor-1 (CR1), membrane cofactor protein (MCP, CD46) and CD59 –which are synthesized by the liver and kidney [54]. It remains unknown in our study whether complement regulatory proteins contribute to the delayed and lessened complement activity in the *In Vivo* setting. In a previous study of limb perfusion followed by replantation, we noticed a sizeable drop in inflammatory and cytokines and complement markers following replantation [55]. Nonetheless, our data are in agreement with previous findings [36, 50].

Moreover, we evaluated the coagulation activity in both models. Analysis of plasma TF concentrations did show no change in both reperfusion settings across all limbs. Studies in heart [56] and renal IRI [57] indicated elsewise, yet our preliminary data remains in agreement

with previously stated findings, and indicating TF plays no role in IRI induced coagulation [50]. In addition, detection of fibrin deposition in tissue revealed no changes at EP across all limbs of both *Ex Vivo* and *In Vivo* setting. This finding is in contrast of previous study results demonstrating tissue fibrin deposition [50]. However, in our previous study, amputated limbs were exposed to 9h of cold ischemia, which could explain the cold-induced fibrin deposition during ischemia time. Similar finding of hypothermia induced fibrin formation was demonstrated in an observational study in humans during cardiopulmonary bypass [58].

A further contributor to reperfusion injury is Von Willebrand Factor as seen by its deleterious role in several IRI animal studies [59-60]. In our study, we observed a measurable increase in vWF among *In Vivo* 9h ischemia limbs after 3h of reperfusion, which supports the delayed and less pronounced IRI indicated by other markers. In *Ex Vivo* limbs, vWF exhibited a sharp drop at the beginning of reperfusion thereafter a rising trend –with higher values in 9h ischemia limbs. The observed drop could be explained by the dilution effect implied by the machine perfusion setup [61]. Furthermore, the contact of blood with machine tubing system not only induces the release of vWF [62], but also promotes coagulation and consumption of coagulation factors [61].

Several studies of IRI have been conducted in different species including small and large animal models [12, 29, 36]. In this and previous studies, we opted for a porcine animal model – owing to its physiological and anatomical similarities to humans– in order to mimic the clinical setting and synthesize translational evidence.

6 Conclusion & limitations

In the present study, our preliminary findings proposes the feasibility of both reperfusion settings to detect limb IRI in a large animal model after prolonged warm ischemia-time. In previous studies, our attempts to reperfuse amputated limbs using the *Ex Vivo* setting –after a duration of 12hr cold ischemia– deemed unsuccessful [36, 50]. To our knowledge, this is the first *Ex Vivo* and *In Vivo* large animal model of limb IRI following a protracted (9h) of warm ischemia time.

One limitation of this study is the absence of skeletal muscle functional evaluation. Moreover, our replantation protocol lacked axial nerve reattachment. As stated by the Chinese surgeons in 1973 "survival without restoration of function is not success" [4]. Furthermore, the use of whole anti-coagulated blood, not only amplifies the damage induced by IRI, but also implies a technical challenge to acquire in remote settings. However, the use of autologous blood was proven superior by Ozer K et al up-to 24h of perfusion [63]. Nonetheless –to overcome this

limitation, other perfusates have been developed for organ transplantation [64], and may be used as substitution including University of Wisconsin [65].

This study opens new avenues to test different protective strategies and pharmacotherapies (e.g. C1-Inhibitor) in order to prolong the time-window between limb amputation until replantation, and improve the success of limb salvage.

7 Outlook

Remaining *In Vivo* experiments and full analysis are warranted to draw a better comparison in regard to both reperfusion settings.

8 Acknowledgement

9 References

1. Ziegler-Graham K, MacKenzie EJ, Ephraim PL, Travison TG, Brookmeyer R. Estimating the prevalence of limb loss in the United States: 2005 to 2050. Arch Phys Med Rehabil. 2008 Mar;89(3):422-9. doi: 10.1016/j.apmr.2007.11.005.
    PMID: 18295618.
2. Østlie K, Skjeldal OH, Garfelt B, Magnus P. Adult acquired major upper limb amputation in Norway: prevalence, demographic features and amputation specific features. A population-based survey. Disabil Rehabil. 2011;33(17-18):1636-49.
    doi: 10.3109/09638288.2010.541973. Epub 2010 Dec 22. PMID: 21174629.
3. Beris AE, Soucacos PN, Malizos KN, Mitsionis GJ, Soucacos PK. Major limb replantation in children. Microsurgery. 1994;15(7):474-8.
    doi: 10.1002/micr.1920150708. PMID: 7968477.
4. Replantation surgery surgery in China. Report of the American Replantation Mission to China. Plast Reconstr Surg. 1973 Nov;52(5):476-89. PMID: 4583285.
5. Maricevich M, Carlsen B, Mardini S, Moran S. Upper extremity and digital replantation. Hand (N Y). 2011;6(4):356-363. doi:10.1007/s11552-011-9353-5
6. Iglesias M, Serrano A. Replantation of amputated segments after prolonged ischemia. Plast Reconstr Surg. 1990 Mar;85(3):425-9. doi: 10.1097/00006534-199003000-00016. PMID: 2304993.
7. i FC, Chang YL, Chen HC, Chuang CC. Three successful digital replantations in a patient after 84, 86, and 94 hours of cold ischemia time. Plast Reconstr Surg 1988;82:346–50.
8. Lin CH, Aydyn N, Lin YT, Hsu CT, Lin CH, Yeh JT. Hand and finger replantation after protracted ischemia (more than 24 hours). Ann Plast Surg. 2010 Mar;64(3):286-90. doi: 10.1097/SAP.0b013e3181b0bb37. PMID: 20179474.
9. Chiu HY, Chen MT. Revascularization of digits after thirty-three hours of warm ischemia time: a case report. J Hand Surg Am. 1984 Jan;9A(1):63-7. doi: 10.1016/s0363-5023(84)80186-0. PMID: 6693746.
10. Nayak, Bibhuti & Mohanty, Rasmi. (2020). Immediate Revascularisation of Borderline Ischemic Limbs Followed by Replantation. 10.21276/ijcmr.2019.6.5.28.
11. Cowled P, Fitridge R. Pathophysiology of Reperfusion Injury. In: Fitridge R, Thompson M, editors. Mechanisms of Vascular Disease: A Reference Book for Vascular Specialists [Internet]. Adelaide (AU): University of Adelaide Press; 2011.
12. Jones, Robert. "An Address On Volkmann's Ischaemic Contracture, With Special Reference To Treatment." The British Medical Journal, vol. 2, no. 3536, 1928, pp. 639–642., www.jstor.org/stable/25330211. Accessed 31 Aug. 2021.
13. Kalogeris T, Baines CP, Krenz M, Korthuis RJ. Cell biology of ischemia/reperfusion injury. Int Rev Cell Mol Biol. 2012;298:229-317. doi: 10.1016/B978-0-12-394309-5.00006-7. PMID: 22878108; PMCID: PMC3904795.
14. Cowled PA, Leonardos L, Millard SH, Fitridge RA. Apoptotic cell death makes a minor contribution to reperfusion injury in skeletal muscle in the rat. Eur J Vasc Endovasc Surg. 2001 Jan;21(1):28-34. doi: 10.1053/ejvs.2000.1209. PMID: 11170874.
15. Willms-Kretschmer K, Flax MH, Cotran RS. The fine structure of the vascular response in hapten-specific delayed hypersensitivity and contact dermatitis. Lab Invest. 1967 Sep;17(3):334-49. PMID: 6051014.
16. Pober JS. Warner-Lambert/Parke-Davis award lecture. Cytokine-mediated activation of vascular endothelium. Physiology and pathology. Am J Pathol. 1988 Dec;133(3):426-33. PMID: 2462353; PMCID: PMC1880803.
17. Hunt BJ, Jurd KM. Endothelial cell activation. A central pathophysiological process. BMJ. 1998;316(7141):1328-1329. doi:10.1136/bmj.316.7141.1328
18. Schlag MG, Harris KA, Potter RF. Role of leukocyte accumulation and oxygen radicals in ischemia-reperfusion-induced injury in skeletal muscle. Am J Physiol Heart Circ Physiol. 2001 Apr;280(4):H1716-21. doi: 10.1152/ajpheart.2001.280.4.H1716. PMID: 11247784.

19. Eppihimer MJ, Lipowsky HH. Effects of leukocyte-capillary plugging on the resistance to flow in the microvasculature of cremaster muscle for normal and activated leukocytes. Microvasc Res. 1996 Mar;51(2):187-201. doi: 10.1006/mvre.1996.0020. PMID: 8778574.

20. Iwahori Y, Ishiguro N, Shimizu T, Kondo S, Yabe Y, Oshima T, Iwata H, Sendo F. Selective neutrophil depletion with monoclonal antibodies attenuates ischemia/reperfusion injury in skeletal muscle. J Reconstr Microsurg. 1998 Feb;14(2):109-16. doi: 10.1055/s-2007-1000152. PMID: 9524329.

21. Kanwar S, Smith CW, Kubes P. An absolute requirement for P-selectin in ischemia/reperfusion-induced leukocyte recruitment in cremaster muscle. Microcirculation. 1998;5(4):281-7. PMID: 9866119.

22. Lozano DD, Kahl EA, Wong HP, Stephenson LL, Zamboni WA. L-selectin and leukocyte function in skeletal muscle reperfusion injury. Arch Surg. 1999 Oct;134(10):1079-81. doi: 10.1001/archsurg.134.10.1079. PMID: 10522850.

23. Stotland MA, Kerrigan CL. E- and L-selectin adhesion molecules in musculocutaneous flap reperfusion injury. Plast Reconstr Surg. 1997 Jun;99(7):2010-20. doi: 10.1097/00006534-199706000-00030. PMID: 9180725.

24. Paoni NF, Peale F, Wang F, Errett-Baroncini C, Steinmetz H, Toy K, Bai W, Williams PM, Bunting S, Gerritsen ME, Powell-Braxton L. Time course of skeletal muscle repair and gene expression following acute hind limb ischemia in mice. Physiol Genomics. 2002 Dec 3;11(3):263-72. doi: 10.1152/physiolgenomics.00110.2002. Epub 2002 Dec 3. PMID: 12399448.

25. Szade A, Grochot-Przeczek A, Florczyk U, Jozkowicz A, Dulak J. Cellular and molecular mechanisms of inflammation-induced angiogenesis. IUBMB Life. 2015 Mar;67(3):145-59. doi: 10.1002/iub.1358. Epub 2015 Apr 21. PMID: 25899846.

26. Mathern DR, Heeger PS. Molecules Great and Small: The Complement System. Clin J Am Soc Nephrol. 2015 Sep 4;10(9):1636-50. doi: 10.2215/CJN.06230614. Epub 2015 Jan 7. PMID: 25568220; PMCID: PMC4559511.

27. Weiser MR, Williams JP, Moore FD Jr, Kobzik L, Ma M, Hechtman HB, Carroll MC. Reperfusion injury of ischemic skeletal muscle is mediated by natural antibody and complement. J Exp Med. 1996 May 1;183(5):2343-8. doi: 10.1084/jem.183.5.2343. PMID: 8642343; PMCID: PMC2192547.

28. Chan RK, Ding G, Verna N, et al. IgM binding to injured tissue precedes complement activation during skeletal muscle ischemia-reperfusion. J Surg Res. 2004;122(1):29-35. doi:10.1016/j.jss.2004.07.005

29. Austen WG Jr, Zhang M, Chan R, et al. Murine hindlimb reperfusion injury can be initiated by a self-reactive monoclonal IgM. Surgery. 2004;136(2):401-406. doi:10.1016/j.surg.2004.05.016

30. Chan RK, Verna N, Afnan J, et al. Attenuation of skeletal muscle reperfusion injury with intravenous 12 amino acid peptides that bind to pathogenic IgM. Surgery. 2006;139(2):236-243. doi:10.1016/j.surg.2005.05.028

31. Sheu EG, Oakes SM, Ahmadi-Yazdi C, Afnan J, Carroll MC, Moore FD Jr. Restoration of skeletal muscle ischemia-reperfusion injury in humanized immunodeficient mice. Surgery. 2009;146(2):340-346. doi:10.1016/j.surg.2009.06.010

32. Zhang M, Alicot EM, Chiu I, et al. Identification of the target self-antigens in reperfusion injury. J Exp Med. 2006;203(1):141-152. doi:10.1084/jem.20050390

33. Shi T, Moulton VR, Lapchak PH, Deng GM, Dalle Lucca JJ, Tsokos GC. Ischemia-mediated aggregation of the actin cytoskeleton is one of the major initial events resulting in ischemia-reperfusion injury. Am J Physiol Gastrointest Liver Physiol. 2009;296(2):G339-G347. doi:10.1152/ajpgi.90607.2008

34. Zhang M, Takahashi K, Alicot EM, et al. Activation of the lectin pathway by natural IgM in a model of ischemia/reperfusion injury. J Immunol. 2006;177(7):4727-4734. doi:10.4049/jimmunol.177.7.4727

35. Chan RK, Ibrahim SI, Takahashi K, et al. The differing roles of the classical and mannose-binding lectin complement pathways in the events following skeletal muscle ischemia-reperfusion. *J Immunol*. 2006;177(11):8080-8085. doi:10.4049/jimmunol.177.11.8080

36. Constantinescu MA, Knall E, Xu X, et al. Preservation of amputated extremities by extracorporeal blood perfusion; a feasibility study in a porcine model. *J Surg Res*. 2011;171(1):291-299. doi:10.1016/j.jss.2010.01.040

37. Bongoni AK, Lanz J, Rieben R, Banz Y. Development of a bead-based multiplex assay for the simultaneous detection of porcine inflammation markers using xMAP technology. Cytometry A. 2013;83(7):636-647. doi:10.1002/cyto.a.22287

38. Chenoweth DE, Cooper SW, Hugli TE, Stewart RW, Blackstone EH, Kirklin JW. Complement activation during cardiopulmonary bypass: evidence for generation of C3a and C5a anaphylatoxins. N Engl J Med. 1981 Feb 26;304(9):497-503. doi: 10.1056/NEJM198102263040901. PMID: 7453783.

39. Wu AH, Perryman MB. Clinical applications of muscle enzymes and proteins. Curr Opin Rheumatol. 1992 Dec;4(6):815-20. PMID: 1457275.

40. Wang X, Sathe AA, Smith GR, Ruf-Zamojski F, Nair V, Lavine KJ, Xing C, Sealfon SC, Zhou L. Heterogeneous origins and functions of mouse skeletal muscle-resident macrophages. Proc Natl Acad Sci U S A. 2020 Aug 25;117(34):20729-20740. doi: 10.1073/pnas.1915950117. Epub 2020 Aug 13. PMID: 32796104; PMCID: PMC7456122.

41. Bosurgi L, Manfredi AA, Rovere-Querini P. Macrophages in injured skeletal muscle: a perpetuum mobile causing and limiting fibrosis, prompting or restricting resolution and regeneration. Front Immunol. 2011 Nov 16;2:62. doi: 10.3389/fimmu.2011.00062. PMID: 22566851; PMCID: PMC3341990.

42. Shireman PK, Contreras-Shannon V, Ochoa O, Karia BP, Michalek JE, McManus LM. MCP-1 deficiency causes altered inflammation with impaired skeletal muscle regeneration. J Leukoc Biol. 2007 Mar;81(3):775-85. doi: 10.1189/jlb.0506356. Epub 2006 Nov 29. PMID: 17135576.

43. Stroo I, Claessen N, Teske GJ, Butter LM, Florquin S, Leemans JC. Deficiency for the chemokine monocyte chemoattractant protein-1 aggravates tubular damage after renal ischemia/reperfusion injury. PLoS One. 2015 Apr 13;10(4):e0123203. doi: 10.1371/journal.pone.0123203. PMID: 25875776; PMCID: PMC4395234.

44. Denk A, Goebeler M, Schmid S, Berberich I, Ritz O, Lindemann D, Ludwig S, Wirth T. Activation of NF-kappa B via the Ikappa B kinase complex is both essential and sufficient for proinflammatory gene expression in primary endothelial cells. J Biol Chem. 2001 Jul 27;276(30):28451-8. doi: 10.1074/jbc.M102698200. Epub 2001 May 3. PMID: 11337506.

45. Akira S, Isshiki H, Nakajima T, Kinoshita S, Nishio Y, Natsuka S, Kishimoto T. Regulation of expression of the interleukin 6 gene: structure and function of the transcription factor NF-IL6. Ciba Found Symp. 1992;167:47-62; discussion 62-7. doi: 10.1002/9780470514269.ch4. PMID: 1385054.

46. Boyle EM Jr, Kovacich JC, Hèbert CA, Canty TG Jr, Chi E, Morgan EN, Pohlman TH, Verrier ED. Inhibition of interleukin-8 blocks myocardial ischemia-reperfusion injury. J Thorac Cardiovasc Surg. 1998 Jul;116(1):114-21. doi: 10.1016/S0022-5223(98)70249-1. PMID: 9671905.

47. De Perrot M, Sekine Y, Fischer S, Waddell TK, McRae K, Liu M, Wigle DA, Keshavjee S. Interleukin-8 release during early reperfusion predicts graft function in human lung transplantation. Am J Respir Crit Care Med. 2002 Jan 15;165(2):211-5. doi: 10.1164/ajrccm.165.2.2011151. PMID: 11790657.

48. Liu L, Shi GP. CD31: beyond a marker for endothelial cells. Cardiovasc Res. 2012 Apr 1;94(1):3-5. doi: 10.1093/cvr/cvs108. Epub 2012 Feb 29. PMID: 22379038.

49. Hoang QT, Nuzzo A, Louedec L, et al. Peptide binding to cleaved CD31 dampens ischemia/reperfusion-induced intestinal injury. Intensive Care Med Exp. 2018;6(1):27. Published 2018 Aug 15. doi:10.1186/s40635-018-0192-3

50. Abdelhafez MM, Shaw J, Sutter D, Schnider J, Banz Y, Jenni H, Voegelin E, Constantinescu MA, Rieben R. Effect of C1-INH on ischemia/reperfusion injury in a porcine limb ex vivo

perfusion model. Mol Immunol. 2017 Aug;88:116-124. doi: 10.1016/j.molimm.2017.06.021. Epub 2017 Jun 20. PMID: 28641140.

51. Subramaniam M, Koedam JA, Wagner DD. Divergent fates of P- and E-selectins after their expression on the plasma membrane. Mol Biol Cell. 1993 Aug;4(8):791-801. doi: 10.1091/mbc.4.8.791. PMID: 7694691; PMCID: PMC300993.

52. Billups KL, Palladino MA, Hinton BT, Sherley JL. Expression of E-selectin mRNA during ischemia/reperfusion injury. J Lab Clin Med. 1995 May;125(5):626-33. PMID: 7537789.

53. Formigli L, Manneschi LI, Adembri C, Orlandini SZ, Pratesi C, Novelli GP. Expression of E-selectin in ischemic and reperfused human skeletal muscle. Ultrastruct Pathol. 1995 May-Jun;19(3):193-200. doi: 10.3109/01913129509064221. PMID: 7543227.

54. Kim DD, Song WC. Membrane complement regulatory proteins. Clin Immunol. 2006 Feb-Mar;118(2-3):127-36. doi: 10.1016/j.clim.2005.10.014. Epub 2005 Dec 9. PMID: 16338172.

55. Müller S, Constantinescu MA, Kiermeir DM, Gajanayake T, Bongoni AK, Vollbach FH, Meoli M, Plock J, Jenni H, Banic A, Rieben R, Vögelin E. Ischemia/reperfusion injury of porcine limbs after extracorporeal perfusion. J Surg Res. 2013 May 1;181(1):170-82. doi: 10.1016/j.jss.2012.05.088. Epub 2012 Jun 17. PMID: 22748598.

56. Mackman N. The role of the tissue factor-thrombin pathway in cardiac ischemia-reperfusion injury. Semin Vasc Med. 2003 May;3(2):193-8. doi: 10.1055/s-2003-40677. PMID: 15199482.

57. Matsuyama M, Yoshimura R, Akioka K, Okamoto M, Ushigome H, Kadotani Y, Nakatani T, Yoshimura N. Tissue factor antisense oligonucleotides prevent renal ischemia-reperfusion injury. Transplantation. 2003 Sep 15;76(5):786-91. doi: 10.1097/01.TP.0000079630.68668.C2. PMID: 14501854.

58. Blombäck M, Kronlund P, Aberg B, Fatah K, Hansson LO, Egberg N, Moor E, Carlsson K. Pathologic fibrin formation and cold-induced clotting of membrane oxygenators during cardiopulmonary bypass. J Cardiothorac Vasc Anesth. 1995 Feb;9(1):34-43. doi: 10.1016/s1053-0770(05)80053-9. PMID: 7718753.

59. Ono, S., Matsui, H., Noda, M. et al. Functional regulation of von Willebrand factor ameliorates acute ischemia-reperfusion kidney injury in mice. Sci Rep 9, 14453 (2019). https://doi.org/10.1038/s41598-019-51013-2

60. Urisono Y, Sakata A, Matsui H, Kasuda S, Ono S, Yoshimoto K, Nishio K, Sho M, Akiyama M, Miyata T, Okuchi K, Nishimura S, Sugimoto M. Von Willebrand Factor Aggravates Hepatic Ischemia-Reperfusion Injury by Promoting Neutrophil Recruitment in Mice. Thromb Haemost. 2018 Apr;118(4):700-708. doi: 10.1055/s-0038-1636529. Epub 2018 Apr 4. PMID: 29618155.

61. Jaime L B, Brandon E Cwan, Madelyn D K, Heidi M B. The Fate of Von Willebrand Factor Concentrate During Cardiopulmonary Bypass: A Case Report. J Anest & Inten Care Med. 2019; 8(3): 555739. DOI: 10.19080/JAICM.2019.08.555739

62. Valen G, Blombäck M, Sellei P, Lindblom D, Vaage J. Release of von Willebrand factor by cardiopulmonary bypass, but not by cardioplegia in open heart surgery. Thromb Res. 1994 Jan 1;73(1):21-9. doi: 10.1016/0049-3848(94)90050-7. PMID: 8178310.

63. Ozer K, Rojas-Pena A, Mendias CL, Bryner BS, Toomasian C, Bartlett RH. The Effect of Ex Situ Perfusion in a Swine Limb Vascularized Composite Tissue Allograft on Survival up to 24 Hours. J Hand Surg Am. 2016 Jan;41(1):3-12. doi: 10.1016/j.jhsa.2015.11.003. PMID: 26710728.

64. Hameed AM, Laurence JM, Lam VWT, Pleass HC, Hawthorne WJ. A systematic review and meta-analysis of cold in situ perfusion and preservation of the hepatic allograft: Working toward a unified approach. Liver Transpl. 2017 Dec;23(12):1615-1627. doi: 10.1002/lt.24829. Epub 2017 Nov 8. PMID: 28734125; PMCID: PMC5725662.

65. Southard JH, van Gulik TM, Ametani MS, Vreugdenhil PK, Lindell SL, Pienaar BL, Belzer FO. Important components of the UW solution. Transplantation. 1990 Feb;49(2):251-7. doi: 10.1097/00007890-199002000-00004. PMID: 1689516.